

SOL-GEL PROCESSING OF ORGANICALLY MODIFIED ITO THIN FILMS
AND CHARACTERIZATION OF THEIR OPTOELECTRONIC AND
MICROSTRUCTURAL PROPERTIES

A THESIS SUBMITTED TO
THE GRADUATE SCHOOL OF NATURAL AND APPLIED SCIENCES
OF
MIDDLE EAST TECHNICAL UNIVERSITY

BY

MEHMET TUMERKAN KESIM

IN PARTIAL FULFILLMENT OF THE REQUIREMENTS
FOR
THE DEGREE OF MASTER OF SCIENCE
IN
METALLURGICAL AND MATERIALS ENGINEERING

JULY 2012

Approval of the thesis:

**SOL-GEL PROCESSING OF ORGANICALLY MODIFIED ITO THIN
FILMS AND CHARACTERIZATION OF THEIR OPTOELECTRONIC AND
MICROSTRUCTURAL PROPERTIES**

submitted by **MEHMET TÜMERKAN KESİM** in partial fulfillment of the requirements for the degree of **Master of Science in Metallurgical and Materials Engineering Department, Middle East Technical University** by,

Prof. Dr. Canan ÖZGEN
Dean, Graduate School of **Natural and Applied Sciences**

Prof. Dr. C. Hakan GÜR
Head of Department, **Metallurgical and Materials Eng.**

Assoc. Prof. Dr. Caner DURUCAN
Supervisor, **Metallurgical and Materials Eng. Dept., METU**

Examining Committee Members:

Prof. Dr. Vedat AKDENİZ
Department of Metallurgical and Materials Eng., METU

Assoc. Prof. Dr. Caner DURUCAN
Department of Metallurgical and Materials Eng., METU

Assoc. Prof. Dr. Arcan DERİCİOĞLU
Department of Metallurgical and Materials Eng., METU

Assoc. Prof. Dr. Burcu Akata KURÇ
Department of Micro and Nanotechnology, METU

Assist. Prof. Dr. Hüsnü Emrah ÜNALAN
Department of Metallurgical and Materials Eng., METU

Date: 02.07.2012

I hereby declare that all information in this document has been obtained and presented in accordance with academic rules and ethical conduct. I also declare that, as required by these rules and conduct, I have fully cited and referenced all material and results that are not original to this work.

Name, Last name: Mehmet Tümerkan Kesim
Signature:

ABSTRACT

SOL-GEL PROCESSING OF ORGANICALLY MODIFIED ITO THIN FILMS AND CHARACTERIZATION OF THEIR OPTOELECTRONIC AND MICROSTRUCTURAL PROPERTIES

KESİM, Mehmet Tümerkan

Master of Science, Department of Metallurgical and Materials Engineering

Supervisor: Assoc. Prof. Dr. Caner DURUCAN

July 2012, 90 pages

Indium tin oxide (ITO) thin films were formed on glass substrates by sol-gel method. Coating sols were prepared using indium chloride tetrahydrate ($\text{InCl}_3 \cdot 4\text{H}_2\text{O}$) and tin-chloride pentahydrate ($\text{SnCl}_4 \cdot 5\text{H}_2\text{O}$) stabilized in organic solvents (acetylacetone and ethanol). First attempt was to synthesize ITO thin films using *standard/unmodified* coating sols. The effect of calcination treatment in air (300 – 600 °C) and number of coating layer(s) (1, 4, 7 or 10) on optoelectronic properties (electrical conductivity and optical transparency), crystal structure and microstructure of ITO thin films were investigated. In addition, single-layer ITO thin films with optoelectronic properties comparable to multi-layered films were prepared by employing organically *modified coating sols*. Oxalic acid dihydrate (OAD) –a drying/microstructure control agent– addition to standard sol formulation was achieved. The rationale was to improve the optoelectronic properties of ITO films through enhancement in microstructure and

chemical characteristics upon OAD addition. The effects of OAD content in the sol formulation and post-coating calcination treatment on electrical/optical properties of ITO films have been reported. Finally, the effects of post coating drying temperature (100 – 200 °C) and time (10 – 60 min) on optoelectronic and microstructural properties of *OAD-modified ITO* thin films were discussed. Thin films have been characterized by scanning electron microscopy (SEM), x-ray diffraction (XRD), x-ray photoelectron spectroscopy (XPS), ultraviolet-visible (UV-Vis) spectroscopy, fourier transform infrared (FTIR) spectroscopy, atomic force microscopy (AFM) and four-point probe measurement techniques. It was shown that film formation efficiency, surface coverage and homogeneity were all enhanced with OAD addition. OAD modification also leads to a significant improvement in electrical conductivity without affecting the film thickness (45 ± 3 nm). Highly transparent (98 % transmittance in visible region) ITO thin films with a sheet resistance as low as 3.8 ± 0.4 k Ω /sq have been obtained by employing coating sols with optimized OAD amount (0.75 M). The optimum post-coating drying temperature (100 °C) and drying time (10 min) was also determined for 0.75 M OAD-modified ITO thin films.

Keywords: Sol-Gel, ITO, Thin Film, Optoelectronics

ÖZ

ORGANİK OLARAK MODİFİYE EDİLMİŞ SOL-JEL ESASLI ITO İNCE FİLMLERİN ÜRETİMİ VE OPTOELEKTRONİK VE YAPISAL ÖZELLİKLERİNİN KARAKTERİZASYONU

KESİM, Mehmet Tümerkan

Yüksek Lisans, Metalurji ve Malzeme Mühendisliği Bölümü

Tez Yöneticisi: Doç. Dr. Caner DURUCAN

Temmuz 2012, 90 sayfa

Bu çalışma kapsamında indiyum kalay oksit (ITO) ince filmleri cam altlıklar üzerinde oluşturulmuştur. Kaplama solüsyonları, indiyum klorür dörthidrat ($\text{InCl}_3 \cdot 4\text{H}_2\text{O}$) ve kalay klorür beşhidratın ($\text{SnCl}_4 \cdot 5\text{H}_2\text{O}$) organik solüsyonlar içerisinde çözülmesiyle hazırlanmıştır. İlk olarak, *standart/modifiye edilmemiş* kaplama solüsyonları ile ITO ince film oluşturulması denenmiştir. Hava ortamında gerçekleştirilen kalsinasyon işleminin (300 – 600 °C) ve kaplama işlem sayısının (1, 4, 7, ya da 10), ITO ince filmlerin optoelektronik özellikleri (elektriksel iletkenlik ve ışık geçirgenlik), kristal yapısı ve mikroyapısına etkisi incelenmiştir. Buna ek olarak; performans özellikleri çok-katmanlı filmlerle karşılaştırılabilir tek-katman ITO ince filmler, organik olarak *modifiye* edilmiş kaplama solüsyonlarından elde edilmiştir. Bir kurutma/mikroyapı kontrol katkı maddesi olan oksalik asit dihidrat (OAD) standart kaplama solüsyonlarına eklenmiştir. ITO ince filmlerin mikroyapı ve

kimyasal karakteristiğindeki muhtemel iyileşmeler sonucunda filmlerin optoelektronik özelliklerinin OAD eklentisi ile artacağı düşünülmüştür. Sollerdeki OAD miktarının ve kaplama sonrası uygulanan kalsinasyon işleminin ITO ince filmlerin optoelektronik özellikleri üzerine etkisi incelenmiştir. Son olarak, kaplama işlemi sonrası uygulanan kurutma işlemindeki sıcaklığın (100 – 200 °C) ve sürenin (10 – 60 dk) ITO filmlerin elektriksel, optik ve mikroyapı özellikleri üzerine etkisi tartışılmıştır. Filmlerin analitik karakterizasyonları taramalı elektron mikroskobu (SEM), x-ışını kırınım (XRD) yöntemi, x-ışını fotoelektron (XPS) spektroskopisi, ultraviyole-görünür (UV-Vis) spektroskopisi, fourier dönüşüm kızılötesi (FTIR) spektroskopisi, atomic kuvvet mikroskobu (AFM) ve dört-nokta direnç ölçümü ile yapılmıştır. ITO ince filmlerinin; film oluşturma verimi, yüzey kaplanması/tutunması ve homojenliği OAD eklentisi ile arttığı gösterilmiştir. Ayrıca, OAD eklentisi, filmlerin elektriksel özelliklerini arttırarak film kalınlığını önemli ölçüde etkilememiştir (45±3 nm). Yüksek ışık geçirgenliğine (98%, görünür bölgede) ve minimum 3.8±0.4 kΩ/sqr yüzey direncine sahip ITO filmleri, optimize edilmiş OAD miktarı (0.75 M) içeren kaplama solüsyonlarından oluşturulmuştur. OAD (0.75 M) ile modifiye edilmiş ITO ince filmler için optimum kurutma sıcaklığı 100 °C, kurutma süresi ise 10 dakika olarak belirlenmiştir.

Anahtar Kelimeler: Sol-Jel, ITO, İnce Film, Optoelektronik

ACKNOWLEDGEMENTS

First and foremost, I would like to thank Dr. Caner Durucan for his support and guidance throughout my thesis project. I also would like to thank my labmates in Materials Chemistry Laboratory for their help and kindness.

In addition, I would like to thank Dr. İbrahim Çam and İlker Yıldız at METU Central Laboratory for their help in AFM and XPS analyses.

And finally, I would like to thank my parents for their patience and support during my whole life.

TABLE OF CONTENTS

ABSTRACT	iv
ACKNOWLEDGEMENTS	viii
TABLE OF CONTENTS	ix
LIST OF TABLES	xiii
LIST OF FIGURES	xiv
LIST OF ABBREVIATIONS	xviii
CHAPTERS	
1. INTRODUCTION	1
1.1 General Introduction and Rationale of the Thesis.....	1
1.2 Background Information and Literature Review	3
1.2.1 Classification of TCOs	3
1.2.2 High Performance TCOs: Choice of Materials	3
1.2.3 Crystal Structure and Factors Affecting Physical Properties of ITO	6
1.3 Production Methods for ITO Thin Films	10
1.3.1 Magnetron Sputtering	11
1.3.2 Pulsed Laser Deposition	11
1.3.3 Chemical Vapor Deposition	12
1.3.4 Electron-beam Evaporation	12
1.3.5 Chemical Spray Pyrolysis (CSP).....	12
1.3.6 Sol-gel Method	13

1.4 Sol-gel Related Coating Methods	15
1.4.1 Spin Coating	15
1.4.2 Dip Coating	16
1.3.3 Spray Coating	16
1.5 Sol-gel Approaches for Preparation of ITO Coating Sols: Processing Details.	16
1.5.1 Indium and Tin Precursors	16
1.5.2 Stabilizers and Solvents.....	18
1.5.3 Functional Additives	20
1.6 Challenges in the Deposition of High Quality/Performance ITO Thin Films via Sol-gel	22
1.6.1 High Calcination Temperature	22
1.6.2 Film Thickness	25
1.6.3 Microstructural Control	27
1.7 Objective of the Thesis.....	30
1.8 Structure of the Thesis.....	31
2. MATERIALS AND METHODS	32
2.1 Materials.....	32
2.2 Preparation of Coating Sols.....	33
2.2.1 Preparation of Plain ITO Sols	33
2.2.2 Preparation of OAD-modified Sols	34
2.3 Preparation of Glass Substrates.....	35
2.4 Coating and Subsequent Treatments	36
2.5 Material Characterization	36

2.5.1 X-Ray Diffraction Analyses	37
2.5.2 Four-point (4-pt) Probe Resistance Measurements	37
2.5.3 Optical Characterization by UV-Vis Spectroscopy.....	37
2.5.4 Scanning Electron Microscopy Analyses	37
2.5.6 Fourier Transform Infrared Spectroscopy Measurements.....	38
2.5.7 X-ray Photoelectron Spectroscopy (XPS) Analyses	38
 3. STANDARD/CONVENTIONAL ITO SOL-GEL FILMS	 39
 3.1 Effect of Calcination Temperature on Structural, Electrical, Optical and Chemical Properties of 4-layered ITO thin films	 39
3.1.1 XRD Analyses	39
3.1.2 Optical Properties of ITO Films	40
3.1.3 Electrical Properties and Surface Chemistry	42
3.1.4 Microstructure: Morphological Analyses.....	45
 3.2 Effect of Number of Layers on Optoelectronic Properties and Microstructure of ITO Thin Films.....	 49
3.2.1 Electrical Properties: Conductivity	49
3.2.2 Optical Properties: Transmittance	50
3.2.3 Microstructure	51
 4. MODIFIED ITO SOL-GEL FILMS: PART I.....	 53
 4.1 Effect of OAD Addition on Structural, Electrical, Optical and Chemical Properties of ITO Thin Films	 53
4.1.1 Phase Analyses and Chemical Structure	53
4.1.2 Optical Transmittance and Electrical Conductivity	58
4.1.3 Microstructural Properties: Film Formation, Morphology and Thickness..	63
 5. MODIFIED ITO SOL-GEL FILMS: PART II	 69

5.1 Effect of Post Coating Drying Conditions on Performance Properties of OAD-modified ITO Thin Films	69
5.2 Effect of Post Coating Drying Conditions on Microstructure of OAD-modified ITO Thin Films.....	71
6. CONCLUSIONS	78

LIST OF TABLES

Table 2.1 Materials used in this study with chemical purities and formulas. Material suppliers are also indicated.	33
Table 3.1 Approximate surface Si and Na contents (in atomic %) of 4-layered plain ITO thin films as determined by XPS analyses.	44

LIST OF FIGURES

Figure 1.1 Resistivity and toxicity figures of various TCOs [16].....	4
Figure 1.2 The carrier concentration and work function of several TCOs [17].....	5
Figure 1.3 Ball-stick model illustration of (a) In (grey) and O (white) atoms in In_2O_3 unit cell and (b) B-site and (c) D-site indium cations in MO_6 octahedral units. Cation positions and anion vacancies are also indicated (d) for further clarification [19,20].	7
Figure 1.4 Kröger-Vink notation of formation of neutral defects and charge carriers in ITO lattice [20].....	8
Figure 1.5(a) Dip, (b) spin and (c) spray coating methods for the formation of sol-gel derived thin films [46].....	15
Figure 1.6 Typical chelation/coordination mechanism of AcAc molecules with In cations resulting in the formation of a ring-like chelate [77].....	20
Figure 2.1 Flowchart for the preparation of plain ITO sols.	34
Figure 2.2 Flowchart for the preparation of OAD-modified ITO sols.....	35
Figure 3.1 XRD diffractogram of 4-layered ITO thin films calcined at different temperatures (for 50 min).....	40
Figure 3.2 Optical transmittance spectra of 4-layered ITO thin films calcined at different temperatures.	41

Figure 3.3 Sheet resistance with standard deviations of 4-layered ITO thin films prepared from plain ITO sols as a function of calcination temperature.....	42
Figure 3.4 High resolution Si(2p) and Na(1s) XPS spectra of 4-layered ITO thin films calcined at (a) 200, (b) 400 and (c) 600 °C.....	44
Figure 3.5 Top view SEM images of 4-layered ITO thin film surfaces calcined at (a) 300 and (b) 600 °C.....	46
Figure 3.6 Energy dispersive x-ray (EDX) spectra of 4-layered ITO thin films calcined at (a) 300 and (b) 600 °C. Inset reveals the spots where the spectra has been taken.....	48
Figure 3.7 Sheet resistance of ITO thin films with standard deviations calcined at 550 °C as a function of number of layers.....	49
Figure 3.8 Optical transparency of ITO thin films calcined at 550 °C as a function of number of layers.....	50
Figure 3.9 Top view SEM images of (a) single-layer and (b) 4-layered ITO thin films calcined at 550 °C.....	52
Figure 4.1 XRD diffractograms of (a) plain and (b) <i>standard</i> OAD-modified ITO (0.75 M OAD) thin films as a function of calcination (1h, in air) temperature.....	54
Figure 4.2 XRD diffractograms of OAD-modified ITO thin films with different extent of OAD addition after calcination at 550 °C (1 h, in air).....	55
Figure 4.3 FTIR transmittance spectra of plain and <i>standard</i> OAD-modified (0.75 M OAD), ITO thin films in as-dried (at 100 °C, 10 min) state.....	56
Figure 4.4 Optical transmittance spectra of (a) plain and (b) OAD-modified ITO (0.75 M OAD) thin films as a function of calcination temperature.....	59

Figure 4.5 Sheet resistance with standard deviations of (a) plain and (b) <i>standard</i> OAD-modified ITO (0.75 M OAD) thin films as a function of calcination (1h, in air) temperature.....	60
Figure 4.6 Sheet resistance with standard deviations of OAD-modified ITO thin films with different extent of OAD addition after calcination at 550 °C (1 h, in air).	62
Figure 4.7 Representative cross-section SEM images of (a) plain and (b) <i>standard</i> OAD-modified ITO (0.75 M OAD) thin films calcined at 550 °C (1 h, in air). The surface images at low magnification for (c) plain ITO and (d) <i>standard</i> OAD-modified ITO (0.75 M OAD) thin films. High magnification images of (e) white regions and (f) gray/black regions on plain ITO surfaces are also indicated.....	64
Figure 4.8 Representative top-view SEM images of (a) 0.1, (b) 0.3, (c) 0.75 and (d) 1 M OAD-modified ITO thin films after calcination at 550 °C (1 h, in air).....	65
Figure 4.9 AFM images of (a) plain and (b) <i>standard</i> OAD-modified ITO (0.75 M OAD) thin films obtained in tapping mode. The average surface roughness values were determined as 8 ± 0.1 nm and 4 ± 0.1 nm, respectively.....	66
Figure 5.1 Optical transmittance spectra of single-layer ITO thin films dried at (a) 100, (b) 125, (c) 175 and (d) 200 °C for 10, 30, and 60 min.	70
Figure 5.2 Sheet resistance of single-layer modified-ITO thin films dried at (a) 100 , (b) 125, (c) 175 and (d) 200 °C for 10, 30, and 60 min.	71
Figure 5.3 Representative SEM images of the surface of the modified-ITO thin films at high magnification (160kx) dried at (a) 100, (b) 125, (c) 175 and (d) 200 °C.	72
Figure 5.4 Representative SEM images of the surface of the modified-ITO thin films dried at 100 °C for (a) 10 min, (b) 60 min. and at 175°C for (c) 10 min, (d) 60 min.	73

Figure 5.5 Representative top view SEM images of the surface of the single-layer OAD-modified thin films at low magnification (1000x) dried at 100 °C for (a) 10 and (b) 60 min at 175°C for (c) 10 and (d) 60 min at 200 °C for (d) 10 and, (e) 60 min. 76

LIST OF ABBREVIATIONS

<i>Abbreviation</i>	
4-pt	Four point
AcAc	Acetylacetone
AFM	Atomic force microscopy
CSP	Chemical spray pyrolysis
CTAB	Cetyl trimethylammonium bromide
CVD	Chemical vapor deposition
DEA	Diethanolamine
DETA	diethylene glycol
EDX	Energy dispersive x-ray
EtOH	Ethanol
FTIR	Fourier transform infrared
GB	Grain boundary
ITO	Indium tin oxide
JCPDS	Joint Committee on Powder Diffraction Standards
kΩ, kOhm	Kilo ohm
MEA	Monoethanolamine
MPTS	Mercaptopropyl trimethoxy silane
Oxalic acid dihydrate	OAD
PC	Polycarbonate
PE	Polyethylene
PEG	Polyethylene glycol
PLD	Pulsed laser deposition
PMMA	Polymethylmetacrylate
PVP	Polyvinylpyrrolidone
RTA	Rapid thermal annealing
SEM	Scanning electron microscopy
SLS	Soda-lime-silicate
TCO	Transparent conductive oxide
TEA	Triethanolamine
UV	Ultraviolet
UV-Vis	Ultra violet visible
XPS	X-ray photoelectron spectroscopy
XRD	X-ray diffraction

CHAPTER 1

1. INTRODUCTION

1.1 General Introduction and Rationale of the Thesis

The first investigation of a transparent conductive oxide (TCO) material dates back to the beginning of 1900s when a film of cadmium metal was oxidized upon heating and became conductive [1]. Since then, TCOs have been studied extensively especially for the last 30 years due to their optical transparency and high electrical conductivity. Owing to their unique characteristics, TCOs have been utilized in various applications such as solar cells, touch screens [2,3], display devices [4], heatable and thermally insulator glasses [5], electrochromic devices [6], electromagnetic [7], and antistatic [8] shielding purposes.

The biggest market that relies on TCOs is display devices. Flat panel displays have been utilized in many fields such as displays in televisions, computers, home appliances and consumer electronics. Depending on the type of the display, conductive electrodes can address each pixel or a larger zone on the display. However, the main function of TCO in all cases is the same. It should be noted that very high conductivity is demanded in order to fabricate energy-efficient screens with fast response [9].

In architectural applications, TCO films have been used in smart windows such as low-emittance (low-e) windows preventing radiative heat losses originating from one side of the window. It is especially important to keep indoors warm in cold climates or vice versa. Moreover, the glass is a poor conductor of heat and has small heat capacity. In cold weather conditions, glass surfaces exposed to atmosphere may drop below the dew point before any other objects in cars and buildings. Therefore, water condensation takes places on the surface of the glass, which may also be accompanied by the formation of frost. Low-e windows are actually beneficial to prevent radiative losses; therefore, inhibiting condensation. Additionally, electrochromic (EC) windows depend heavily on TCO industry. TCOs enable electrical charge insertion and extraction in the EC layer; therefore, they are an essential component in coloring and bleaching of the smart windows. Last but not the least, heat build-up occurs in conductive glasses when an electric current passed through it which is useful in deicing of glass panels [3,5,8].

The general objective of this thesis was to *establish sol-gel processing routes to fabricate ITO thin films* on SLS glass substrates of nominal composition. Currently, mass production of ITO films in industry requires expensive vacuum-based coating methods such as sputtering. In this thesis, sol-gel method was chosen as an alternative processing technique due to its simplicity and low-cost. Moreover, special emphasis was also given to deposit *single-layer films (< 100 nm in thickness)* in order to eliminate tedious multiple coating and drying cycles that are conventionally employed in literature in making ITO through sol-gel routes. In this respect, this work offers some novel and original contribution to the 20 some-yearlong research efforts along this line, i.e. fabricating ITO by sol-gel routes. The proposed and modified processing approach of this study aims *improvement in electrical performance* of the ITO thin films through certain microstructural/morphological and chemical improvements.

1.2 Background Information and Literature Review

1.2.1 Classification of TCOs

TCOs can be categorized depending on the type of the charge carriers (holes or electrons) and the amount of components that form the oxide phase (unary, binary, multicomponent). There are three main types of TCOs. The first group is the wide band gap n-type semiconductor oxides, which include fluorine doped tin oxide ($\text{SnO}_2:\text{F}$, FTO), $\text{SnO}_2:\text{Sb}$, tin doped indium oxide ($\text{In}_2\text{O}_3:\text{Sn}$, ITO), $\text{In}_2\text{O}_3:\text{Mo}$, aluminium doped zinc oxide ($\text{ZnO}:\text{Al}$, AZO), gallium doped zinc oxide ($\text{ZnO}:\text{Ga}$, GZO), indium doped zinc oxide ($\text{ZnO}:\text{In}$) [4,9,10]. These materials have the best optoelectronic performance among TCOs. Resistivities on the order of $10^{-4} \Omega\text{cm}$ were reported for GZO and FTO thin films. On the other hand, best AZO and ITO thin films were shown to have resistivities as low as $10^{-5} \Omega\text{cm}$ [4,11]. The second group of TCOs consists of multicomponent oxides such as $\text{In}_4\text{Sn}_3\text{O}_{12}$, ZnSnO_3 , $\text{Zn}_2\text{In}_2\text{O}_5$, $\text{In}_4\text{Sn}_3\text{O}_{12}$, GaInO_3 , Zn_2SnO_4 , MgIn_2O_4 and $\text{Zn}_2\text{In}_2\text{O}_5$. Resistivities reported for these materials are on the order of $10^{-2} \Omega\text{cm}$ to $10^{-4} \Omega\text{cm}$ [4,12,13]. The final group of TCOs consists of p-type semiconductor oxides including CuAlO_2 , SrCu_2O_2 , CuGaO_2 , and AgInO_2 [14]. One important approach to utilize highly conducting p-type TCOs is to combine these materials with n-type TCOs in order to fabricate p-n junctions solely with TCOs. However, p-type TCOs inherently have lower conductivities due to their electronic structure [15]. All in all, n-type binary semiconductor TCOs stand out because of their high electrical performance.

1.2.2 High Performance TCOs: Choice of Materials

Although there has been a great effort to synthesize and develop novel TCOs to achieve low resistivity and high optical transparency values, ITO still remains as an indispensable material among all TCOs. Figure 1.1 compares the resistivity and toxicity figures of several TCOs. It can be seen that indium oxide (In_2O_3), zinc oxide (ZnO), and cadmium oxide (CdO) based doped n-type semiconductors exhibit

Binary	Dopant	Resistivity	Toxicity
ZnO	Al, Ga, B, In, Y, Sc, V, Si, Ge, Ti, Zr, Hf, // F	⊙	
CdO	In, Sn	⊙	××
In ₂ O ₃	Sn, Ge, Mo, Ti, Zr, Hf, Nb, Ta, W, Te // F	⊙	×
Ga ₂ O ₃	Sn	Δ	
SnO ₂	Sb, As, Nb, Ta // F	○	
TiO ₂	Nb, Ta	Δ	
Ternary			
MgIn ₂ O ₄		Δ	
GaInO ₃ , (Ga, In) ₂ O ₃	Sn, Ge	Δ	
CdSb ₂ O ₆	Y	Δ	×
SrTiO ₃	Nb, La	×	
Ternary			
Zn ₂ In ₂ O ₅ , Zn ₃ In ₂ O ₆	Multi-component ZnO–In ₂ O ₃ system	○	
In ₄ Sn ₃ O ₁₂	In ₂ O ₃ –SnO ₂ system	○	
CdIn ₂ O ₄	CdO–In ₂ O ₃ system	○	×
Cd ₂ SnO ₄ , CdSnO ₃	CdO–SnO ₂ system	○	×
Zn ₂ SnO ₄ , ZnSnO ₃	ZnO–SnO ₂ system	Δ	
	ZnO–In ₂ O ₃ –SnO ₂ system	○	
	CdO–In ₂ O ₃ –SnO ₂ system	○	×
	ZnO–CdO–In ₂ O ₃ –SnO ₂ system	○	×

: ⊙Very good, ○: Good, Δ: Average, ×: Bad, ××: Very bad.

Figure 1.1 Resistivity and toxicity figures of various TCOs [16].

exceptional resistivities when compared to rest of the semiconductor oxides. FTO has also good electrical properties with low emissivity in near-IR, which makes this material attractive for low-emissivity windows [8]. CdO based TCOs pose a significant health and environmental risk due to high toxicity of cadmium; therefore, cannot compete with In₂O₃ (specifically ITO) and ZnO (specifically AZO) based TCOs. Among them, ITO stands out not only for its excellent electrical properties, but also due to its high stability in acid and alkali environments and high temperature oxidation resistance. ZnO is vulnerable to etching and chemical attack in traditional lithographic processes due to its instability in acidic mediums/solutions. Additionally, it is susceptible to oxidation which makes a processing challenge and deterioration in conductivity was observed for oxidized films [1,4].

Figure 1.2 shows the carrier concentration and work function (energy required to move an electron from Fermi level into vacuum) of several TCOs. It can be seen that plain and doped In_2O_3 thin films have higher number of charge carriers than ZnO-based oxides leading to higher conductivities. Oxygen vacancies in plain In_2O_3 lattice

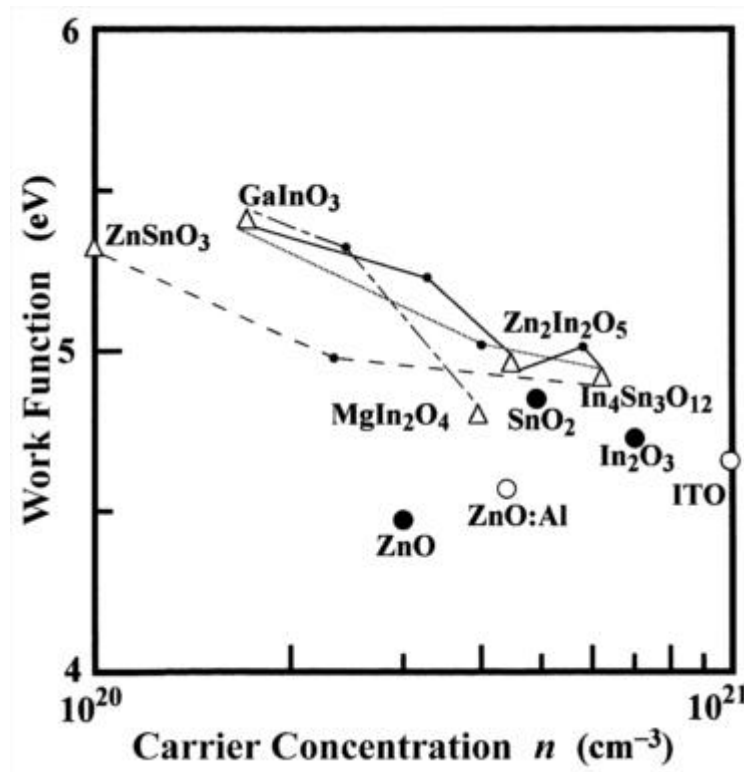


Figure 1.2 The carrier concentration and work function of several TCOs [17].

generate two free electrons, whereas only one free electron is produced in ZnO. Consequently, concentration of carriers in ZnO-based thin films is inherently lower when compared to In_2O_3 -based films. Therefore, it is more difficult to synthesize ZnO-based thin films that have comparable electrical performance to In_2O_3 -based films [4]. In general, ITO thin films have high IR reflectance, good electrical conductivity, good substrate wetting and compatibility, high hardness and chemical

inertness [18]. For the aforementioned reasons, ITO thin films have notable advantages and importance in industry over other TCOs.

1.2.3 Crystal Structure and Factors Affecting Physical Properties of ITO

1.2.3.1 Crystal Structure of ITO

In_2O_3 in crystalline form has a cubic bixbyite structure and hosts 80 atoms in its unit cell. Due to its unique crystal structure, it can accommodate large number of defects. As mentioned earlier, two oxygen atoms are missing in its atomic configuration (*Section 1.2.2*); therefore two electrons are produced for charge compensation/neutrality. Figure 1.3 shows the crystal structure of In_2O_3 and anion vacancies (Figure 1.3b-c and Figure 1.3d) in the unit cell. The crystal structure of In_2O_3 is similar to fluorite. The cations (Ca^{2+}) in fluorite are distributed in face centered translations in which all tetrahedral interstitial sites are occupied by fluorine ions. Fluorite has MO_8 (M: metal) coordination units forming a cube. Oxygen ions reside on the edges of the cube and a metal cation sits next to the center of the cube. On the other hand, in In_2O_3 lattice, two oxygen atoms are missing either in body (Figure 1.3b, B-site) or face (Figure 1.3c, D-site) diagonals, which results in the formation of MO_6 octahedron units. In these units, indium atoms are repelled slightly from the center. This configuration causes formation of two different non-equivalent indium sites in the unit cell. It should be emphasized that non-equivalent nature of indium sites stems from the occupancy of oxygen atoms at different sites shifting the position of indium atoms due to electrostatic interaction [19].

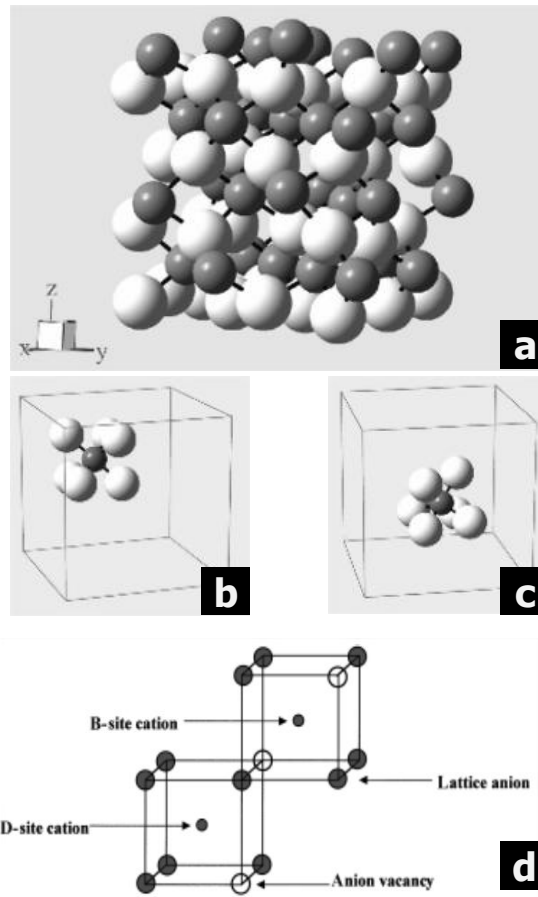


Figure 1.3 Ball-stick model illustration of (a) In (grey) and O (white) atoms in In₂O₃ unit cell and (b) B-site and (c) D-site indium cations in MO₆ octahedral units. Cation positions and anion vacancies are also indicated (d) for further clarification [19,20].

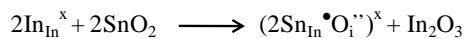
1.2.3.2 Charge Carrier Generation Mechanisms in ITO Thin Films

The generation of charge carriers both intrinsic (in In₂O₃ lattice) and extrinsic (due to dopant atoms) can be shown in Figure 1.4 using Kröger-Vink notation. Figure 1.4 also includes one of the neutral defects that may be reduced to generate charge carriers and contribute to conductivity. Scattering mechanisms and types of defects are discussed in detail in *Section 1.2.3.3*. It can be seen from Figure 1.4 that oxygen vacancies in ITO lattice generate intrinsic charge carriers. If In₂O₃ lattice is doped with Sn⁺⁴, tin atoms may substantially be incorporated as defects and due to charge neutrality requirements a free electron must be produced. Moreover, if ITO film

contains a neutral defect, under some circumstances (e.g. reducing atmosphere), these defect complexes may be reduced and tin atoms may reside in In_2O_3 lattice, therefore generating carriers. The electrical conductivity of ITO thin films actually arises from the presence of defects in the structure. It should be noted that carrier generation mechanisms of other TCOs are similar to that of ITO.

A degenerate semiconductor can be synthesized if the concentration of the dopant atoms is relatively higher. In a degenerate semiconductor, fermi level overlaps with the conduction band resulting in metal-like conductivity without displaying absorption in the visible range of light spectrum (400 – 700 nm). If the amount of carriers increases in a degenerate semiconductor, fermi level shifts to a higher position in the conduction band. Consequently, the energy required to move an electron from valance band to conduction band should be increased, and this increase would be proportional to the amount of degeneracy *i.e.* the amount of charge carriers. This is known as the Burstein-Moss effect and it widens the band gap of degenerate semiconductors [21,22].

Neutral Defects



Carrier Generation

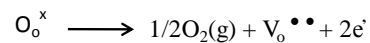


Figure 1.4 Kröger-Vink notation of formation of neutral defects and charge carriers in ITO lattice [20].

1.2.3.3 Electron Scattering Mechanisms in TCO Thin Films

There are several electron scattering mechanisms observed in TCOs which deteriorate the electron mobility. It is worth to mention that there are contradictory interpretations in the literature about the dominant scattering mechanisms that deteriorates the electrical properties in TCOs. Scattering mechanisms observed in all TCOs are quite similar to each other.

First of all, grain boundaries (GBs) are believed to be one of the major scattering factors. It is suggested that grain boundaries host oxygen atoms and/or molecules. These species gather electrons from the conduction band and render negatively charged. Electrons must travel through these potential barriers/depletion layers; therefore, their mobilities are diminished. The decrease in the conductivity is more pronounced for films having larger potential barrier (higher negative charge on GB surface). However, it was also indicated that GB scattering becomes dominant when the crystal size is small (comparable to mean free path of electron) and/or the carrier concentration is low [22,23]. Minami [16] compared the electrical resistivities of AZO and GZO films in atmospheres having different humidity levels. He concluded that formation of depletion layers at the surface of GBs are the main reason for the decrease in resistivity rather than scattering of electrons at the GBs especially for thinner films. On the other hand, several authors [24–26] claimed in their studies that increasing the crystallite size of ITO thin films decrease the overall resistivity.

Another proposed scattering mechanism is neutral and ionized impurity scattering. Neutral defects in TCOs are generally originated from excess metallic atoms of the host and/or external dopants. These defects can be ionized or stay in their neutral state. Additionally, host and/or donor atoms may also form defect complexes with oxygen in the structure. Frank and Köstlin [27] reported formation of electrically neutral defect complexes in ITO thin films, which is detrimental for conductivity. Sn^{4+} and Sn^{2+} defect clusters associate to form Sn^{3+} complexes having same valance as In^{3+} . Consequently, no charge carriers can be generated by incorporation of these complexes into In_2O_3 lattice. Moreover, presence of Sn^{2+} and Sn^+ impurity oxide phases in the structure was also reported to decrease conductivities. Warschkow *et*

al. [28] was also supported Frank and Köstlin's findings by reporting that electron scattering phenomenon in ITO thin films emerges mainly from the presence of neutral defects. To the contrary, Zhang *et al.* [23] indicated that the concentration of neutral defect complexes is lower and the scattering cross section is much smaller than ionized impurities. Consequently, they suggest the effect of neutral impurity scattering is negligible for plain and doped oxide thin films. Their study shows that ionized impurity scattering dominates at low temperature, whereas at elevated temperatures, phonon scattering becomes prevalent. There are also other studies on different TCOs, such as AZO [4], CdO [22], ZnO and FTO [23] reporting that the prevalent scattering centers are ionized impurities. Another study points the effect of ionized impurities on electron mobilities of ITO thin films [29]. The authors also observed a decrease in electron mobilities at high doping concentrations. They conclude that electron-electron scattering may dominate and/or some neutral defect complexes can be formed at high doping levels. Tomonaga *et al.* [30] also observed a decrease in the conductivity of ITO thin films upon increasing dopant concentration. They concluded that free electrons interact with each other and therefore decrease their mobilities.

Additionally, at higher temperatures, the number of phonons in the lattice increases and hinders electron movement. It should also be emphasized that GB scattering can be neglected when the crystal size of ITO films is larger than the mean free path of the electrons. Finally, high amount of dopant in TCO films triggers the electron scattering mechanism and decrease the conductivities. Nevertheless, from the aforementioned studies, neutral and ionized impurity scattering mechanisms seem to control the electron mobilities of TCOs more than any other proposed mechanism.

1.3 Production Methods for ITO Thin Films

Optical, electrical and morphological properties of ITO thin films rely heavily on the production method. Considering the importance of ITO thin films in big markets such as FPDs and solar cells, the performance of ITO thin films is of paramount importance. It is also crucial to find a method which is simple and low cost.

Commercial ITO thin films are produced mainly by sputtering. There are several methods to deposit ITO thin films such as magnetron sputtering [31], pulsed laser deposition (PLD) [32], CVD [33], e-beam evaporation [34], chemical spray pyrolysis (CSP) [35], pechini method [36] and sol-gel method [24]. The features of these methods are discussed in the following subsection. It should be indicated that the almost exponentially escalating prices and limited availability of indium sources pushes all the research efforts towards economical ITO thin film deposition methods.

1.3.1 Magnetron Sputtering

In sputtering method, a target material is bombarded with high energy ions to knock atoms and/or molecules from the target to form thin films on various substrates. ITO thin films have been produced commercially by sputtering techniques. The disadvantage of sputtering methods is the requirement of high vacuum during processing and the inefficient use of ITO targets, which increase the cost of production. There are various types of sputter deposition systems. Among them, magnetron sputtering is the most widely employed version in general and specifically for the deposition of ITO thin films. Magnetron sputtering differs from direct current (DC) sputtering in terms of utilization of lower voltages and pressures. Additionally, higher deposition rates can be achieved during processing. It has been shown many times that sputtered ITO thin films show higher performance compared to other deposition methods [37–39].

1.3.2 Pulsed Laser Deposition

Pulsed laser deposition (PLD) technique is a variant of evaporation methods. Even though its usage is currently limited to laboratory scale, PLD is capable of producing multicomponent films with good stoichiometry control. In order to evaporate atoms/molecules/ions on the surface of the target, a laser and a series of lenses are utilized to focus beams. The transferred energy is then transformed into chemical, mechanical and thermal energy knocking out the moieties on the surface of the target. Evaporated species condense on the film surface and form thin films. It should be emphasized that PLD method is ineffective in terms of energy output/input ratio.

Moreover, high initial cost associated with setting up a PLD system makes it an expensive method for the production of ITO thin films [40,41].

1.3.3 Chemical Vapor Deposition

Chemical vapor deposition (CVD) is a method of thin film deposition through transferring reactive volatile species of a material in the gas phase onto the substrate to be coated. Gas phase constituent should condense on the surface of the substrate – not in the chamber– in order to avoid powder formation by homogeneous nucleation instead of thin films. Activation of the reaction can be triggered by means of applying electric field, sending electrons or simply by heating. Unlike sputtering, CVD processes can be performed at atmospheric and low pressures and more affordable in terms of operation and equipment costs. In this method, a variety of metallic, organic, inorganic and semiconductor materials can be prepared with high stoichiometry control [40,41].

1.3.4 Electron-beam Evaporation

Electrons are emitted from a high energy electron gun and directed onto the target material to be used for deposition. Electrons produce heat upon impact with surface atoms/molecules of the target. High purity films with little or no contamination can be prepared and coating rates are higher when compared to sputtering methods. On the other hand, non-uniform evaporation on the surface of the target may lead to problems in controlling the thickness and prevents formation of uniform films. Additionally, this technique also requires vacuum, increasing the cost of deposition [41].

1.3.5 Chemical Spray Pyrolysis (CSP)

CSP is a simple solution based approach for the deposition of metallic or semiconducting thin films. A spray solution is prepared by dissolving the precursors of interest in a solvent. Then the spray solution is atomized by means of a pneumatic, electrostatic force, ultrasonic waves and or corona discharge. The atomized droplets

leave the nozzle and travel through the surface of the heated substrate. Volatiles and solvents are evaporated, forming thin solid films. The amount of dopant, deposition rate and the thickness of thin films can be precisely controlled [42]. On the other hand, diluted spray solutions and slow spraying rates should be used in order to improve the film quality, which may increase the duration of the coating process. In addition to this, CSP is sensitive to a variety of parameters; most important of all is temperature. Temperature variations on the substrate surface may result in local differences in physical, electrical and optical properties of thin films, thereby decreasing the quality of the prepared films [43].

1.3.6 Sol-gel Method

In sol-gel method of deposition of thin films, precursors of metal alkoxides and metal salts are dissolved in appropriate solvents (alcohols, water) to form the sol. In addition, sols may contain some additives such as stabilizers to coordinate metal cations in order to improve chemical homogeneity. The reactions leading to formation of oxide network commence firstly by the hydrolysis of alkoxide chains. Hydrolysis reaction can be accompanied by condensation of hydrolyzed moieties (M-OH, M: metal) to form the oxide skeleton (M-O-M). Generally, for the production of thin films by sol-gel method, condensation reactions leading to formation of a xerogel network are desired following the deposition of hydrolyzed sols in order to ensure good coverage. The sols should contain sufficient amount of hydroxyl (-OH) groups to facilitate good adhesion onto glass and silicon substrates, which contain plenty of hydroxyl groups on their surface after subjected to appropriate cleaning procedures. Some of the examples of application areas of sol-gel method include but not limited to optical coatings, electronic films, porous films and protective films. Reflective and antireflective coatings alter the physical state of glass and change the optical properties. By applying an electric current to an electrochromic film, it is possible to change the transmittance of glasses. TCOs render the glass conductive while maintaining high optical transparency. Ferroelectric and superconductive thin films can also be prepared by sol-gel method. Sol-gel protective coatings impart strength, corrosion resistance and abrasion

resistance to improve material properties. Sol-gel derived highly porous films can be utilized in sensor applications. Moreover, high surface to volume ratio catalyst and filter products can be synthesized by sol-gel technique [44].

One feature of sol-gel method is the ability to synthesize highly pure and homogeneous products by employing simple and low cost coating techniques. It is feasible to coat large or complex-shaped substrates by sol-gel method. Additionally, solutions with precise amount of dopants can be prepared easily without the need for expensive equipments (e.g. high vacuum chambers). Moreover, manipulation of sol chemistry at the atomic scale by use of different precursors, solvents, and additives enable researchers to improve the optoelectronic properties of ITO thin films. By controlling the microstructure, crystallization behavior, chemical homogeneity and thickness of ITO thin films, the optoelectronic properties can be improved. Additionally, low processing temperatures make sol-gel method suitable for industrial scale production. Moreover, sol-gel method not only enables the deposition of thin films, but also monoliths, fibers and powders can be produced.

On the other hand, there are also some drawbacks/limitations associated with sol-gel method. Organic alkoxide precursors are quite expensive and sensitive to changes in temperature and moisture content of processing atmosphere. This problem can be avoided if metal salts are used in processing instead of alkoxides. Moreover, the density of films is generally lower when compared to vacuum methods such as sputtering. The residual pores in the films may deteriorate the functional and structural properties of films and coatings, except porous films [45]. Nevertheless, sol-gel method enables researchers and industrialists to produce a wide variety of products through relatively simple and cheap processes. In these respects, ITO thin film deposition through sol-gel method has attracted numerous researchers and resistivities comparable to that of sputtered films can be obtained.

1.4 Sol-gel Related Coating Methods

Figure 1.5 shows the representative schematics for film formation methods generally used in sol-gel processing of thin films. Coating techniques can be categorized into three groups, namely spin, dip and spray coating.

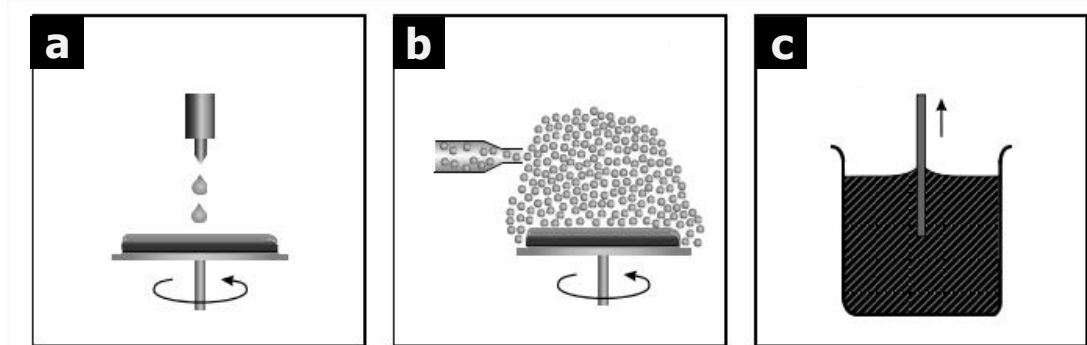


Figure 1.5 (a) Dip, (b) spin and (c) spray coating methods for the formation of sol-gel derived thin films [46].

1.4.1 Spin Coating

In spin coating, sols are poured on a substrate placed on the vacuum chuck of a spinner. After that, substrate and the chuck is rotated at the desired speed for pre-determined durations. The excess solvent is driven off due to centrifugal forces. Sols adhere onto the substrate accompanied by evaporation of volatiles/organics. Desired film thickness can be obtained depending on the viscosity and surface tension of the coating sol, centrifugal speed and duration of spinning. Moreover, it is feasible to obtain multi-layered films by repeating the procedure. The major drawback of this technique is the requirement of a flat substrate [47].

1.4.2 Dip Coating

Dip coating is the immersion of the substrate to be coated into the coating solution which is followed by either drawing the substrate from solution or drawing the reaction vessel away from the substrate to deposit thin films. During substrate removal, organics and water are evaporated leading to the formation of a thin film. Dip coating technique is advantageous in terms of allowing the coating complex-shaped substrates such as hollow, concave and convex pieces. Additionally, both sides of the substrates can be coated simultaneously. The thickness of the deposits depends on the viscosity and density of the solution and the withdrawal speed. Dipping technique can be continuous or batch, both of which are fully adaptable to large scale manufacturing [44,47].

1.3.3 Spray Coating

Spray coating uses a gun that sprays a dilute coating solution onto the substrate. Atomized droplets form films on the substrate surface. This method is utilized to coat intricate features and substrates when a high film quality is not a prerequisite. Solvent properties such as boiling point (determines evaporation rate) and substrate wetting are important parameters. Spray coating enables fast processing and is more flexible in terms of possibility of coating complex-shaped substrates. Furthermore, since low solution volumes are used for spraying, it is an efficient process in terms of raw materials utilization. Additionally, substrate and the solution do not have a physical contact, eliminating the risk of contamination of the solution by the substrate [47,48].

1.5 Sol-gel Approaches for Preparation of ITO Coating Sols: Processing Details

1.5.1 Indium and Tin Precursors

Precursors for the preparation of ITO solutions can be broadly categorized into three groups. Organic precursors; namely metal alkoxides have been used to prepare ITO coating solutions. Indium isopropoxide ($\text{In}_2\text{O}(\text{OC}_3\text{H}_7)_3$) and tin-t-butoxide ($\text{Sn}(\text{OC}_4\text{H}_9)_4$) [49]; indium acetate ($\text{In}(\text{CH}_3\text{COO})_3$) and tin octylate ($\text{Sn}(\text{C}_8\text{H}_{17}\text{O})_2$)

[25]; indium propoxide ($\text{In}(\text{OC}_3\text{H}_7)_3$) and tin propoxide ($\text{Sn}(\text{OC}_3\text{H}_7)_4$) [50–52] are some examples of organic precursors used in the literature to form coating sols. Although the purity of alkoxides is high, higher costs associated with the synthesis and limited availability of alkoxides restrict the utilization of organic precursors in ITO sols. Additionally, ITO sols prepared from organic precursors are extremely sensitive to humidity and temperature, thus limiting the shelf life and industrial applicability of these sols. Moreover, some of the organic precursors are inflammable (e.g. acetates). Furthermore, it was found that although it is possible to dissolve high amount of indium ions in alkoxide route enabling the synthesis of single-layer films with appreciable thickness, the resistivity of these films are still high [18,25].

Indium and tin metal salts are attractive alternatives to organic precursors. Indium chloride (InCl_3) and indium chloride tetrahydrate ($\text{InCl}_3 \cdot 4\text{H}_2\text{O}$) based solutions can be doped with stannic chloride (SnCl_4) [53–56], stannous chloride dihydrate ($\text{SnCl}_4 \cdot 2\text{H}_2\text{O}$) [57,58] and stannous chloride pentahydrate ($\text{SnCl}_4 \cdot 5\text{H}_2\text{O}$) [24,59]. Additionally, indium nitrate ($\text{In}(\text{NO}_3)_3 \cdot x\text{H}_2\text{O}$ ($x=0,3,5$)) based solutions can be used in conjunction with tin chloride precursors mentioned above. Moreover, there are also studies in the literature utilizing indium and tin metal ingots as starting materials for obtaining ITO thin films. However, pure metal precursors can also be considered as “metal salts” due to dissolving them either in nitric or hydrochloric acid before tin doping [24,60–62]. The high availability of inorganic metal salts and their lower cost when compared to alkoxides makes them preferred precursors for the deposition of ITO thin films. ITO sols of metal salts are highly resistant to gelation and their shelf life is notably longer. On the other hand, solubility of metal salts in organic solvents is rather limited; therefore coating sols should be prepared with low indium concentration. Solution concentration/molarity determines the thickness of ITO thin films, so films prepared from inorganic precursors are thinner. In order to synthesize films with sufficient thickness (200 – 250 nm) to obtain reasonable conductivities, multiple coating approaches are needed to be adapted, which makes processing rather tedious [18,24,54].

The nature of the precursors dictate the nature of coating solutions and significantly affect the microstructure, optical and electrical properties and crystallization characteristics of the resultant ITO thin films. It was reported that thin films prepared from nitrate-based indium precursors have higher amount of charge carriers, wider optical band gap and higher conductivity compared to films deposited from chloride-based precursors [63]. It was also reported that residual chlorine affects the uniformity of ITO thin films [64]. However, it should be strongly emphasized that impurities from inorganic precursors lowers the conductivity of films. Additionally, in order to remove chlorine (Cl⁻) and nitrate (NO₃⁻) ions, films should be calcined at higher temperatures (600 °C). These ions not only deteriorate the conductivity of films, but also increase the calcination temperature determined by the onset of crystallization [65].

The final group of ITO thin film precursors is crystallized ITO nanoparticles. Instead of using a sol-gel approach, colloidal films can be synthesized by preparing a colloidal solution of nanoparticles stabilized in appropriate solvents [7,25,66–69]. Colloidal solutions can be dip or spin coated to form single-layered ITO films with sufficient thickness. Moreover, using crystalline nanoparticles, thermally-induced crystallization step is excluded during deposition offering low temperature processing. Low temperature deposition is important in terms of utilization of polymeric substrates especially for flexible electronic applications. However, thick nanoparticulate films inherently contain open pores and have low-density, which inhibit electron transport and increase the surface roughness of ITO thin films.

1.5.2 Stabilizers and Solvents

The role of solvents in solution-based processing approaches is mainly providing a reaction medium for constituents. Moreover, solvents control the initiation and rate of some molecular level reactions. Some of the important solvent characteristics are polarity, boiling point, density, viscosity and molecular weight. All of these properties determine the nature of solution and subsequent film formation and drying characteristics. The solvents used in the synthesis of ITO thin films by sol-gel

method are typically acetylacetone [55], alcohols (methanol, ethanol, propanol, etc.) [49], acetylacetone-alcohol mixtures [70] and ethylene glycol [18].

Stabilizers and chelating agents are frequently employed in the synthesis of ITO thin films by sol-gel method. The major role of a chelating agent is to promote chemical homogenization of the solution by coordinating metal cations in their molecular structure. Therefore, distribution of metal cations in solution leads to the formation of films with high degree of chemical homogeneity and improved performance. The second role of a chelating agent is to decrease the chemical reactivity of metal cations, in other words suppressing the degree of hydrolysis and condensation reactions. This is especially important for alkoxide precursors since their high reactivity can be a major problem leading to precipitation due to high degree of condensation during deposition of films [6,71].

For sol-gel processing of ITO thin films, several chelating agents such as short-chain carboxylates (e.g. acetic acid) [72], β -diketones (e.g. acetylacetone) [70], monoethanolamine (MEA) [73], diethanolamine (DEA) [25], triethanolamine (TEA) [18], diethylene triamine (DETA) [74] were used. Among them, acetylacetone (2,4-pentanedione, AcAc) has proven to be a versatile stabilizer for indium ions. AcAc forms a ring like chelate with indium ions and stabilize them in solutions. It should be noted that, many studies in the literature uses AcAc as a chelating agent and also as a solvent. The main reason for using AcAc for such dual functionality is the potential in increasing the chelation efficiency and in increasing the solubility of the chelate to improve the chemical homogeneity [75]. AcAc comprised of enol and keto forms in equilibrium mixture. It has various coordination modes and it can form monodentate (metal cation bonding with one oxygen) and bidentate chelates (metal cation bonding with two oxygens). In basic solutions, it can be deprotonated to form acetylacetonato anion, which is also a ligand to bind metal cations [76]. Figure 1.6 shows the representative configuration of a bidentate In-AcAc chelate.

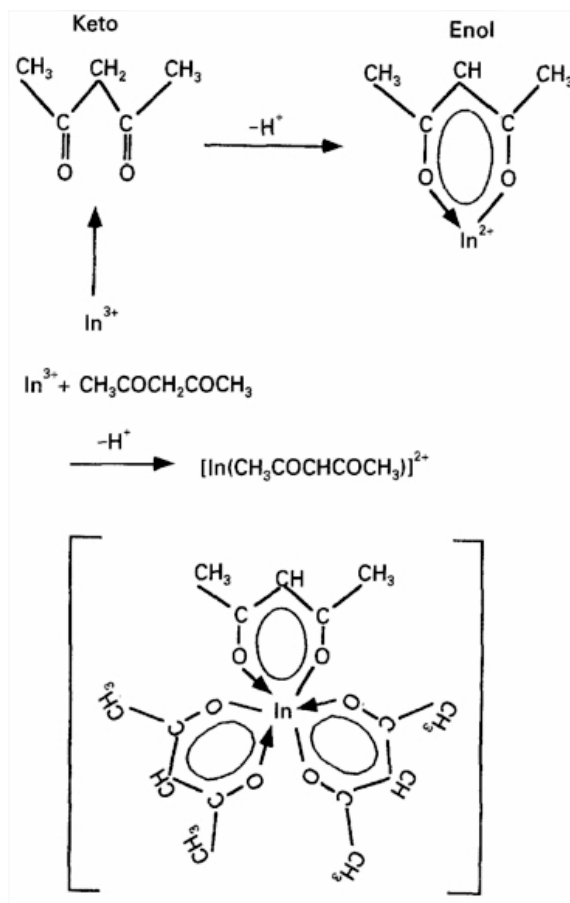


Figure 1.6 Typical chelation/coordination mechanism of AcAc molecules with In cations resulting in the formation of a ring-like chelate [77].

1.5.3 Functional Additives

There have been several reports on fabricating ITO thin films through the use of modified coating solutions with additives to impart different properties to the resultant thin films. It should be noted that most of these additives are organic compounds. The additives that were used in ITO solutions can be categorized into three groups. The first group consists of surfactants that are employed in order to change the structural and morphological properties of ITO thin films. Additives in the second group are utilized intentionally to form porous films. Film forming agents and binders are also used in the preparation of colloidal ITO thin films.

Zhang *et al.* used polyethylene glycol (PEG) in sol formulations to deposit ITO thin films. They observed that PEG forms smoother, crack-free films with lower surface roughness when compared to unmodified films. Moreover, PEG doped solutions are more stable. PEG addition also alters the optical and structural properties of ITO films. They reported that optical transmission of PEG-doped films is increased whereas crystal quality is diminished [78]. Liu and his co-workers investigated the effect of additives on performance properties of their ITO thin films. They used MEA, PEG and MEA+PEG to modify the coating solutions. They claimed that addition of MEA changes the crystal orientation of films, which in turn increases the optical transmission. Furthermore, additives also change the microstructural properties of the films. In their study, various types of the surfactants are used significantly to change the grain size and surface morphology of ITO thin films [59].

Additives in the second group are templating agents employed to form mesoporous films with controlled porosity. It should be emphasized that low-density and porous films are required for catalytic, sensor and filtering applications as mentioned earlier in *Section 1.3.6*. The pore size and distribution depend on the type of templating agent utilized. Studies reporting the use of cetyl trimethylammonium bromide (CTAB) [79,80] and block co-polymers [81,82] as templating agents can be found in the literature to form porous ITO thin films.

ITO nanoparticulate films have porous nature as indicated previously in *Section 1.5.1*, which decreases their functional properties. Königer *et al.* prepared ITO/PVP nanocomposites employing colloidal film forming methods. They used PVP as an additive to improve film forming characteristics of ITO. They reported that addition of PVP increases the conductivity of ITO thin films and impart good mechanical properties. Moreover, they also observed that PVP is a good film forming agent preventing formation of cracks [83]. Maksimenko *et al.* synthesized nanoparticulate ITO films by adding PVP and mercaptopropyl trimethoxy silane (MPTS) into coating solutions. They indicated that scratch resistance and adhesion of films with additives is higher than that of plain ITO thin films. They argued that during drying, PVP glues the nanoparticle network together to form denser and more compact films.

On the other hand, MPTS which was used as a binder also increases the density of films. When treated with ultraviolet (UV) light, MPTS begins to polymerize leading to a dense 3-D network [84]. Aegerter *et al.* used 3-GPTS and 3-MPTS in sol formulations as binders to form thick (500 nm), single-layer ITO thin films at a process temperature of 130 °C. They reported sheet resistance values as low as 8 kOhm/sqr under UV-irradiation/crystallization.

The reported examples clearly reveal the ability to control the microstructure of ITO films with additives processed by solution-based approaches. Resultant microstructural improvements affect the performance properties of the films positively.

1.6 Challenges in the Deposition of High Quality/Performance ITO Thin Films via Sol-gel

There are some important problems/limitations associated with the deposition of ITO films by sol-gel method. The remedies to some of these problems are actually the main objective of this thesis. This section describes these problems in detail and some of the solutions reported in the literature by various researchers.

1.6.1 High Calcination Temperature

As-deposited, sol-gel deposited ITO thin films generally require a calcination step to induce crystallization and exclude organic compounds present in the as-dried state. Annealing temperature is dictated by the nature of the sols, *i.e.* type of In and Sn precursors, solvents and additives. Crystalline films have higher transparency and electrical conductivity when compared to amorphous ITO thin films. Generally, a calcination process performed above 300 °C is required to obtain reasonable performance properties for sol-gel derived ITO thin films prepared from inorganic metal salts as precursors [85]. Optimum calcination temperature was reported to be around 550 °C for sol-gel derived ITO thin films that gives the best optoelectronic performance as indicated by numerous researchers [18,58,72]. Relatively higher calcination temperatures not only increase the cost of processing of ITO thin films,

but also limit the use of organic substrates such as polycarbonate (PC), polyimide, polymethylmetacrylate (PMMA) and polyethylene (PE). Utilization of organic substrates is essential in flexible electronic applications, especially in flexible display devices.

Additionally, several researchers claimed that high temperature calcination deteriorates the electrical properties of ITO thin films due to diffusion of highly mobile cations from the SLS glass substrates into the films. It was reported that, even though the crystallinity improves with calcination, a heat treatment at temperatures in excess of 550 °C is expected to lower the electrical conductivity, due to cation (Na^+ , Ca^{2+} , etc.) exchange from underlying glass substrates [24]. In order to overcome this problem, barrier layers are deposited underneath the ITO layers. Many studies report on the use of silica (SiO_2) as a barrier layer in order to improve the electrical properties of ITO thin films through the prevention of the diffusion of alkali ions [60,62,86]. Lee *et al.* [86] reported a decrease in the conductivity of ITO thin films through calcination for longer than 20 min even at 400 °C. However, deposition of a SiO_2 barrier layer complicates the process and increase the cost. Alternative solution to this problem is to utilize glass substrates that do not contain alkali ions, such as quartz and borosilicate.

In order to decrease the calcination temperature, various attempts have been made by researchers. One approach is to prepare hybrid sols. In this method of deposition, powdered crystalline ITO nanoparticles are added into solutions prepared by conventional sol-gel processes. The role of crystalline nanoparticle addition is to introduce seed particles into sols in order to lower the crystallization temperature of the resultant film. Thermal analysis data show that it is feasible to lower the crystallization temperature by 10 °C [50]. Hong *et al.* [87] prepared organic ITO sols and added 0.6 wt % ITO nanoparticles with respect to total weight of the sols. They obtained single-layer ITO films with resistivities down to 7000 Ω at approximately around 83 % transmittance at a calcinations temperature of 500 °C. Toki *et al.* [50] also prepared organic sols containing ITO nanoparticles. They reported that, resistivities down to 0.3 Ωcm can be obtained using solutions containing 50 wt % ITO

nanoparticles with respect to the total weight of the solution. However, it should be noted that films still exhibit relatively low conductivity and the decrease in crystallization temperature seems to be insufficient for the utilization of organic substrates.

The second approach to lower the calcination temperature of ITO thin films is employing colloidal processing methods to form films solely based on crystalline ITO nanoparticles. Processing steps include: (i) synthesis of ITO nanoparticles, (ii) stabilizing the nanoparticles in suitable solvents/stabilizers to form the colloidal solution and (iii) coating the dispersion by wet coating (spin or dip coating) or printing methods, which also allow the production of patterned ITO films. Various authors reported synthesis of nanoparticulate ITO thin films by spin and dip coating of colloidal dispersions [26,60,66,67,69,88–91]. Although, colloidal processing is a promising approach to lower the calcination temperature, synthesized films inherently have low density reducing the performance properties of these films [69]. Moreover, in the aforementioned studies, as-deposited nanoparticulate ITO films have resistivities on the order of 0.002 – 30 Ωcm . It is worth to mention that such low resistivity values can be obtained only by annealing in a controlled environment either in vacuum or in reducing atmosphere. In addition, colloidal ITO thin films inherently possess significant degree of porosity and poor interparticle contact due to limited packing and sinterability, degrading both electrical and optical performance. It is well-known that annealing of ITO films in an atmosphere devoid of oxygen decreases the resistivity of ITO thin films by increasing oxygen vacancies and reducing the neutral defect complexes mentioned in *Section 1.2.3.2* [24,26,92]. Additionally, some of the authors reported that the sheet resistance of the films increases up to 3 times during storage in air. They claimed that the porous films are saturated with oxygen and thus, some of the oxygen vacancies are filled up resulting in a decrease in the amount of charge carriers [66,67,69]. There are also studies reporting the use of binders (*See Section 1.5.3: Functional Additives*) in order to increase the contact between individual ITO nanoparticles to form denser films with improved electrical properties.

In addition, attempts have been made to prepare sol-gel derived TCO films by the incorporation of metal nanoparticles to form nanocomposite films in order to enhance the conductivity. There are studies on the deposition of silver (Ag)-incorporated SnO₂ [93], Ag-incorporated AZO [94,95] and Ag-incorporated ITO [73] in the literature. Although the rationale behind these studies is to improve electrical properties, it was found that addition of Ag into film matrix enhances the crystal quality of deposited films. Ag nanoparticles acted as seeds favoring the crystallization of the matrix similar to forming hybrid ITO solutions by the addition of ITO nanoparticles mentioned previously in this section. All in all, it is feasible to lower the crystallization temperature of metal-incorporated films provided that metals can be reduced at corresponding calcination temperature.

Another novel and original way of eliminating the adverse effects of high temperature calcinations relies on the UV-laser induced processing of ITO thin films prepared by conventional sol-gel processing routes. Tao *et al.* [96] used chlorides of In and Sn as precursors and employed dip coating to prepare ITO thin films on SiO₂ substrates. Before UV-laser irradiation, a drying operation was conducted at 260 °C. They reported resistivities around 0.0075 Ωcm for 5-layered films. However, the optical properties of their films were not reported. In another study [85], organic precursors of In and Sn were utilized to form ITO films on PET and PC substrates by spin coating. Films were dried at 100 °C. In order to crystallize the film network, multiple laser shots were sent to remove organics from the gel network. The authors indicated that organics in the films were decomposed without shrinkage of the films, therefore, ITO thin films in their study contain significant amount of porosity. However, prepared ITO thin films have resistivity values around 0.063 Ωcm on PET substrates with 10 shots, and 0.031 Ωcm on glass substrates with 100 shots.

1.6.2 Film Thickness

Sol-gel derived, spin or dip coated ITO thin films prepared from inorganic precursors have thickness values in the range of 25 – 40 nm thickness values for a single layer. The amount of charge carriers increases with the thickness of ITO films.

Additionally, scattering of electrons from the film surface becomes more significant and dominant for very thin films; therefore decreasing the carrier mobility. In order to obtain low resistivities, multiple coating approaches should be implemented to form dense ITO thin films with sufficient thickness. The coating-drying or coating-drying-calcination procedures should be repeated several times to obtain ITO films with desired electrical properties. This makes the process impractical [7,59,68]. Many number of coating/drying cycles as high as fifteen [49], twenty [24] or thirty [97] may be required, which is not suitable with the large scale manufacturing practice.

There are various parameters that can affect the thickness of ITO thin films. For instance, increasing the solution molarity of the coating sol in terms of In and Sn amounts would lead to formation of thicker ITO films. Beaurain *et al.* [58] reported that increasing the solution molarity from 0.1 to 0.2 M decreases the sheet resistance of the films higher than two-fold at all calcination temperatures. Yamamoto and his co-workers [98] reported that highly viscous solutions should be utilized in order to increase the thickness of ITO films. It should be noted that spin or dip coating with a concentrated viscous sol would increase the thickness of ITO deposits. However, solubility of the metal salts is rather limited in organic solvents (*See Section 1.5.1: Indium and tin precursors*). As a result of this, the upper limit of solute (In and Sn) concentration is dictated by the solubility of In and Sn precursors.

Spin coating parameters are also crucial in controlling the thickness of the resultant films. It was reported that increasing the rotation speed in spin coating results in the formation of thinner films. Films prepared at 1000 rpm have a sheet resistance of 1.5 k Ω /sqr sheet resistance, while films spin coated at 10000 rpm exhibit a sheet resistance of 16 k Ω /sqr. However, it was also indicated that high rotation speeds result in denser and more homogeneous films with better optical properties [99]. Therefore, a trade-off should be made between electrical and optical performance.

Moreover, coating a thick, single-layer film may result in the formation of cracks. Limited solvent evaporation during drying and calcination steps may result in the

formation of defects in thicker films. Additionally, thermal expansion mismatch between ITO film and the underlying substrate may contribute to the formation of defects especially for thick films [98].

Colloidal film forming approaches as mentioned previously in *Section 1.5.1* and *Section 1.6.1* stand out among other solution-based processing methods (e.g. sol-gel) in terms of forming single-layer films. Thicker films can be prepared with nanoparticle loaded suspensions. Ederth *et al.* [66] deposited colloidal ITO thin films having 220 nm thickness by a two-step calcination method. First step involves calcination of ITO films between 200 – 400 °C for 2h. After that, samples were calcined in air at 500 °C for 2 h. They obtained resistivity values down to 0.1 Ωcm for their ITO films with a transmittance higher than 90 %. In another study reporting the preparation of colloidal films, the authors indicated that colloidal ITO films in their study exhibited a resistivity of 0.015 Ωcm and a transparency around 90 % following calcination at 900 °C. Schwab *et al.* [69] prepared nanoparticulate, dip coated 500 nm ITO films. They achieved film resistivity of 0.0091 Ωcm and a transparency higher than 85 %. Additionally, 600 nm ITO thin films exhibiting transparency around 90 % with resistivity values as low as 0.008 Ωcm was reported [91].

Some other works in the literature report on the preparation of ITO thin films by combining colloidal processing method with UV-laser irradiation. Dahoudi *et al.* [26] prepared colloidal films by UV-induced crystallization. After UV-curing, they heat-treated colloidal films at 130 °C for 13 h and finally applied additional heat treatment under reducing atmosphere to improve the electrical properties of films. They reported resistivities around 0.09 Ωcm for 570 nm thick, single-layer films. It should be noted that substrates coated in this study were PMMA and PC.

1.6.3 Microstructural Control

Sol-gel derived ITO thin films inherently possess considerable amount of porosity. Charge carriers and incident electromagnetic radiation scatter because of these

defects; therefore, optoelectronic performance of ITO thin films may decrease. Microstructure of ITO thin films determines the final performance properties. Grain size, film density, surface roughness and film coverage significantly affect the overall performance of the thin films. These material properties can be controlled by changing the calcination and drying conditions. Additionally, cooling method (furnace or air cooling) employed after calcination may drastically change the microstructure. Last but not the least, heating method used during calcination may affect the final properties. This section presents some of the methods to improve the electrical properties of ITO thin films by altering the microstructure.

Synthesis of a multi-layered film with conventional resistive heating techniques requires a considerable amount of time. It was also indicated that conventionally calcined films have randomly oriented grains with significant amount of porosity. Rapid thermal annealing (RTA) procedures were suggested to decrease the processing times and improve the microstructure of ITO thin films [68,71]. It was reported that ITO thin films prepared by RTA method have higher density than films prepared by conventional heating methods. RTA causes heat build up simultaneously in the entire ITO layer; therefore, nucleated crystallites exhibit narrow grain size distribution. Small and uniform-sized grains in the films were suggested to improve the percolation of ITO grains; therefore, decreasing the amount of porosity. Additionally, enhancement in the density of films prepared by RTA was accompanied with a reduction in thickness. These films were reported to have better electrical properties [68]. Moreover, RTA procedures were reported to improve the surface roughness of the ITO thin films. ITO films calcined by RTA method had an average surface roughness around 0.3 – 1.5 nm which is almost an order of magnitude lower than the surface roughness of conventionally calcined ITO thin films [71].

Microwave heating of ITO thin films was claimed to improve their electrical properties. Microwave heating method is similar to RTA in terms of achieving rapid heating rates. Temperatures on the surface of the substrate can reach 650 °C within 30 min using a commercial kitchen microwave. Chloride precursors of In and Sn can

be decomposed to produce ITO thin films with controlled stoichiometry. Microwave heated 900 nm films were consisted of cubic ITO grains up to 400 nm in size. Film resistivities down to $5 \times 10^{-4} \Omega \text{cm}$ can be achieved by microwave heating. However, films were reported to have a rough surface [100].

Li *et al.* [101] investigated the effect of cooling method right after calcination on the optoelectronic properties of ITO thin films. They reported that denser films with smaller grain sizes can be produced by air cooling. On the other hand, furnace-cooled ITO thin films were found to contain significant amount of porosity. Additionally, they observed that there are In_2O_3 precipitates on the surface of furnace-cooled films. Therefore, cooling method employed in the synthesis may also affect the film uniformity. They stated that grain growth can be suppressed by cooling the films in air. Improvement in film density decreased the resistivity of films. However, transparency of furnace-cooled films was reported to diminish significantly due to formation of microcracks. Instant cooling causes stress build-up in the film and microcracks were formed [101].

Microstructure of the ITO films prepared by sol-gel method depends heavily on the calcination temperature. Change in the morphology of the films is expected due to transition from amorphous to a polycrystalline state having well-defined GBs. However, independent of the degree of crystallization, grain size and surface roughness of ITO films can be drastically changed depending on the calcination temperature used in preparation. Hammad *et al.* [72] stated that increasing the calcination temperature leads to grain growth and improve the electrical properties associated with an increase in the degree of crystallinity. Surface roughness was reported to be increased for the films with larger particles. However, no quantitative information/data was given to support these results. On the other hand, it was also reported that increase in the calcination temperature during processing leads to grain refinement in the film as opposed to observations made by Hammad and his co-workers. Decrease in the surface roughness of the films was correlated with formation of smaller ITO grains at high calcination temperatures [102]. Grain refinement phenomena observed in sol-gel derived ITO films upon increasing

calcination temperature was also reported by other authors [103]. Contradictive results may be seen in the previous studies for the change in particle size with increasing calcination temperature due to differences in the nature of coating sols and the processing parameters used to synthesize ITO thin films. However, it is evident that calcination temperature significantly affects the final microstructure of the films. Finally, it should also be noted that changing the duration of calcination also changes the microstructure of the resultant ITO thin films as indicated by various authors [104,105].

1.7 Objective of the Thesis

The aim of the current study is to address and solve some of the aforementioned problems (*Section 1.6: Challenges in synthesis of high quality/performance ITO thin films via sol-gel*) in obtaining high performance ITO sol-gel thin films. The specific objectives of this work can be outlined as follows:

- Deposition of ITO thin films on glass substrates by sol-gel method using commercial quality/purity In and Sn precursors (metal salts). In parallel, investigation of various processing parameters (calcination temperature (300 – 600 °C) and number of coating layers) on electrical and optical properties of ITO films will be performed in determining the optimum preparation conditions. This part of the thesis can be considered as *standard/conventional* way for developing ITO films by sol-gel. However, this section provides some reference knowledge for subsequent parts of the thesis.
- Deposition of single-layer ITO sol-gel thin films with optoelectronic properties comparable to those of multi-layered sol-gel derived films that are formed by conventional means. This functional improvement will be achieved by establishing a novel modification in the sol formulation through the use of a controlled drying agent (oxalic acid dihydrate, OAD). The effect of *OAD modification* on electrical, optical, and microstructural properties of ITO films will be investigated in a systematic manner and will be compared to those prepared by conventional sol-gel recipes.

- Investigation of selected processing parameter (post coating drying conditions) on electrical, optical and microstructural properties of *OAD-modified ITO thin films*.

-

1.8 Structure of the Thesis

The *first chapter* gives general information about the properties and application areas of TCOs. The importance of ITO as a transparent conductive electrode has been emphasized and the various methods for the preparation of ITO thin films were introduced. After presenting the features and problems of sol-gel derived ITO thin films, the specific objectives of the thesis were also stated in this chapter.

The *second chapter* contains experimental information in regard to preparation of conventional and modified ITO thin films. The materials and details of the experimental procedures are presented. Additionally, details of analytical characterization methods and conditions used to evaluate structural, optical, electrical and morphological properties of ITO thin films are described.

The following three chapters (*Chapter 3, 4, 5*) are the results and interpretation of them, focusing on findings related to the properties of conventional and OAD-modified ITO thin films. An extensive and complete materials characterization was provided in explaining/relating microstructure and optoelectronic properties (electrical conductivity and optical transmittance) of the films with different processing histories.

Sixth chapter summarizes the findings of the thesis. The main conclusions and some ideas for future work are presented.

CHAPTER 2

2. MATERIALS AND METHODS

The chemicals used in this thesis are described in this chapter. Additionally, analytical characterization methods that have been used to evaluate material properties are given.

2.1 Materials

The materials used to prepare plain and modified-ITO coating solutions are listed in Table 2.1. Additionally, suppliers and purity of these materials are also indicated. All chemicals were used as received without any further purification treatment.

Table 2.1 Materials used in this study with chemical purities and formulas. Material suppliers are also indicated.

Material	Supplier	Chemical Formula	Purity
Indium trichloride tetrahydrate	Sigma-Aldrich	$\text{InCl}_3 \cdot 4\text{H}_2\text{O}$	97 %
Tin tetrachloride pentahydrate	Sigma-Aldrich	$\text{SnCl}_4 \cdot 5\text{H}_2\text{O}$	98 %
Acetylacetone	Sigma-Aldrich	$\text{C}_5\text{H}_8\text{O}_2$	> 99 %
Ethanol	Sigma-Aldrich	$\text{C}_2\text{H}_5\text{OH}$	Absolute
Oxalic acid dihydrate	Riedel-de Haën	$\text{C}_2\text{H}_2\text{O}_4 \cdot 2\text{H}_2\text{O}$	> 99.5 %

2.2 Preparation of Coating Sols

The ITO coating solutions prepared by *conventional* sol-gel approaches will be referred as *plain* ITO sols hereafter. The details for preparation of *plain* and *modified-ITO* sols are summarized by the flowcharts given in Figure 2.1 and Figure 2.2, respectively.

2.2.1 Preparation of Plain ITO Sols

For the preparation of plain ITO coating sols, 3.3 g of $\text{InCl}_3 \cdot 4\text{H}_2\text{O}$ was dissolved in AcAc (30 mL) at 25 °C. The In-solution was refluxed at 60 °C using a water bath and condensing tube for 3 h to ensure effective homogenization. The solution was colorless initially. After reflux period, solution turned to dark orange/brown

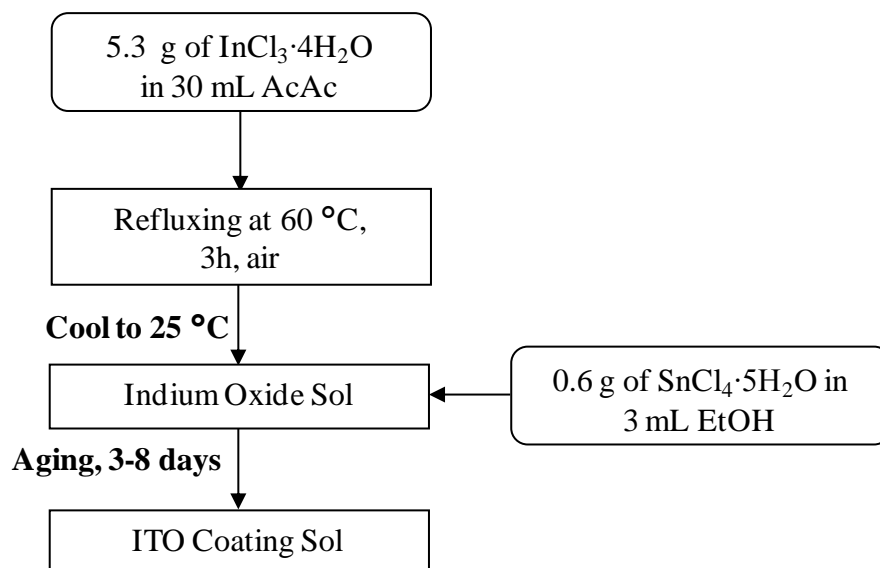


Figure 2.1 Flowchart for the preparation of plain ITO sols.

indicating complexation of indium ions with AcAc molecules. Meanwhile, 0.6 g $\text{SnCl}_4 \cdot 5\text{H}_2\text{O}$ was dissolved in EtOH (3 mL) in another glass beaker with the help of a magnetic stirrer at 25 °C. After refluxing, In-containing solution was cooled to 25 °C and Sn chloride solution was then added dropwise. The final composition of the ITO coating sol was 0.55 M in terms of In content and this specific compositions corresponds to an In/Sn atomic ratio of 10.

2.2.2 Preparation of OAD-modified Sols

The OAD-modified ITO solutions were obtained by adding OAD into the ITO sol prepared by the protocol mentioned in *Section 2.2.1*. The ITO sol was mixed for 20 min before the addition of OAD powder. Then, 4.16 g of OAD was added into the parent ITO sol (a total volume of 44 mL). This corresponds to an OAD molarity of 0.75 M in the final coating sol formulation. This amount of OAD incorporation can be considered as *standard* compositional modification. However, OAD modified ITO sols with various amounts (0.28, 0.56, 1.66, 2.77, 5.55 g) of OAD addition were also prepared to enable a parametric compositional analysis. The other formulations of the modified gels correspond to an OAD molarity of 0.05 – 1.0M; 0.05, 0.1, 0.3,

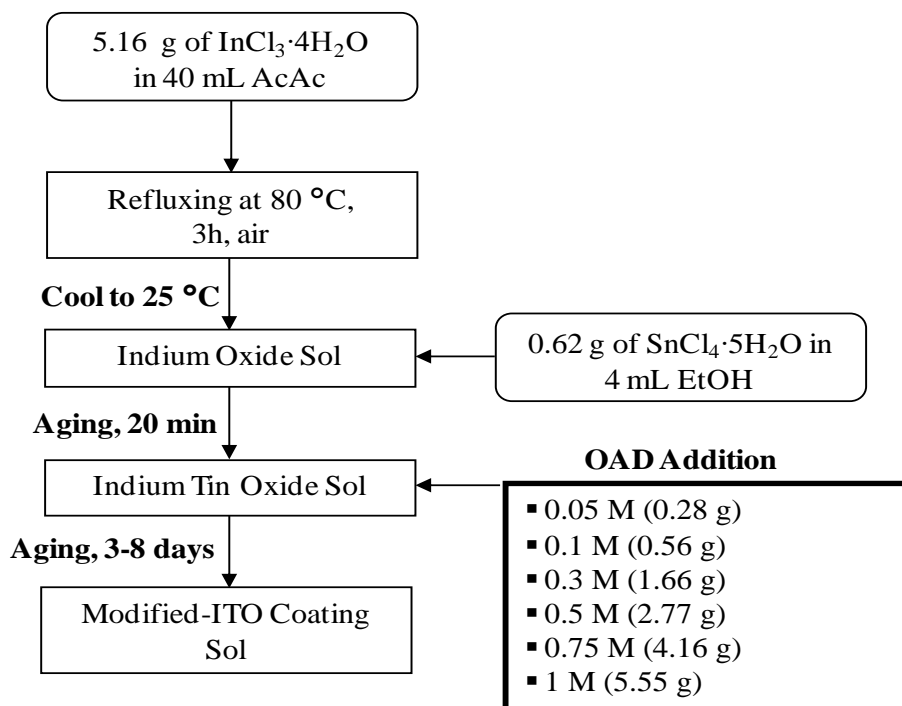


Figure 2.2 Flowchart for the preparation of OAD-modified ITO sols.

0.5 or 1.0 M. OAD addition more than 5.55 g (corresponding 1 M OAD) could not be achieved, because OAD did not dissolve completely in ITO sol. The color of the sols was controlled by the amount of OAD. Plain ITO sols were dark orange/brown which turned gradually into orange upon the addition of OAD. The color change was more distinct and intensified for the higher amount of OAD-added sols.

2.3 Preparation of Glass Substrates

Wet cleaning techniques are essential to remove the dust and contaminants from the glass surface and for the activation of surface hydroxyl groups prior to coating operation. The substrate was soda-lime-silicate (or SLS, precleaned microscope slides, Gold Seal 25×25 mm) glass. The glass substrates were first treated ultrasonically for 20 min in acetone, in EtOH and finally in DI water. The substrates were washed thoroughly with DI water between subsequent cleaning operations and finally rinsed with DI water and dried at 100 °C for 10 min in air after cleaning.

2.4 Coating and Subsequent Treatments

The coating was performed by spin coating using Laurell, WS-400B-6NPP/LITE spin coater. For a typical coating operation, approximately 0.2 mL of coating sol was deposited on the pre-cleaned glass piece by a micropipette. Spinning was performed at 3000 rpm for 30s. Different drying and calcination combinations were used for plain and modified films.

The plain ITO coated samples were dried in an open atmosphere oven at 150 °C for 10 min. The coating/drying cycle was repeated to obtain multilayered films up to four-layer. The films were calcined in air at 300, 400, 500, 550 or 600 °C for 1 h.

The OAD-modified thin films were formed only in single layer form using the same spin coating parameters. The coated sample are typically dried at 150 °C for 10 min and calcined at 300, 400, 500, 550 or 600 °C for 1 h. For the modified films the effect of drying temperature and time was also investigated and drying was also performed at 100, 175 or 200 °C for 10, 30 and 60 min. Films were calcined at 550 °C for 1 h in air.

2.5 Material Characterization

This part of the thesis contains detailed information about analytical characterization methods and characterization conditions used to evaluate material properties of ITO thin films. XRD was used for the phase analysis and to assess the crystallinity of the films. In order to measure the sheet resistance of the thin films, 4-point probe measurement technique was utilized. UV-Vis spectroscopy was used to determine the optical transparency of ITO films. The film coverage and surface morphology was investigated with low and high magnification SEM images respectively. Additionally, cross-sectional SEM images were used to determine the thickness of ITO deposits. AFM images were utilized to determine the microstructure and surface roughness of thin films. Chemical nature of the ITO thin films was determined by FTIR and XPS analyses.

2.5.1 X-Ray Diffraction Analyses

X-ray diffraction (XRD) was used to monitor the transition from amorphous to crystalline state during calcination of ITO thin films. Additionally, it was utilized to determine the relative crystal quality of samples subjected to different processing conditions. Rigaku D/Max-2000 PC model diffractometer was used for analysis. The diffraction tests were performed for diffraction angle (2θ) range of $20 - 65^\circ$, at a scanning rate of $2^\circ/\text{min}$ using Cu-K_α radiation and an operation voltage of 40 kV and a current of 30 mA.

2.5.2 Four-point (4-pt) Probe Resistance Measurements

The sheet resistance values (in $\text{k}\Omega/\text{sqr}$) for thin films were measured using a 4-pt. probe conductivity measurement set-up (Jandel). The sheet resistance values were measured at ten different locations on the same sample and their average and standard deviation values are reported. Standard deviation values in resistance were evaluated as a qualitative indication of the physical homogeneity of the films.

2.5.3 Optical Characterization by UV-Vis Spectroscopy

The optical transmittance of films was investigated by UV-Vis spectrophotometer (Cary100 Bio, Varian). The double beam scanning was used for the measurement of transmittance values for the thin films in the wavelength range of 300 – 800 nm. An uncoated glass substrate was used as a blank reference for baseline correction.

2.5.4 Scanning Electron Microscopy Analyses

The microstructure and thickness of the thin films were examined using a FEI Quanta 400F model field emission scanning electron microscope (FESEM) operated at 10 kV. Additionally, morphological changes were investigated for samples prepared under different processing parameters and from sols having different formulations. The SEM samples were coated with a conductive gold layer by

sputtering prior to SEM analyses. The cross-sectional images shown in this thesis are for the films formed on silicon wafer using identical coating sols and processing parameters.

2.5.5 Atomic Force Microscopy Investigations

Atomic force microscopy (AFM) was used to investigate the effect of OAD-modification on the surface roughness of ITO thin films. Additionally, microstructural details of the films were also examined in order to complement SEM findings. The coating surfaces of selected samples were imaged using VeecoNanoscopeV AFM in Tapping Mode using a silicon sharpened tip (nominal tip radius of 5 –10 nm) at a scan rate of 1 Hz. Multiple scans of 1×1 or 2×2 μm size were captured at multiple locations on the same film surface in order to ensure representative images.

2.5.6 Fourier Transform Infrared Spectroscopy Measurements

Differences in the chemical nature of plain and OAD-modified ITO thin films were inspected by FTIR analyses. The measurements were carried out using a Mid-IR spectrometer (Frontier, PerkinElmer) with attenuated total reflection (ATR) attachment (GladiATR Single Reflection, PIKE). Transmittance spectra of films were acquired in the range 4000 – 400 cm⁻¹ with a resolution of 4 cm⁻¹.

2.5.7 X-ray Photoelectron Spectroscopy (XPS) Analyses

X-ray photoelectron spectroscopy (XPS) analyses were performed to investigate the chemical nature of ITO film surfaces. XPS spectra were obtained using a PHI 5000 spectrometer. High resolution scans for Si (2p) and Na (1s) spectral regions were collected for quantitative analyses of chemical constituents. The binding energies and charge collections were referenced to the C (1s) line at 284.6 eV.

CHAPTER 3

3. STANDARD/CONVENTIONAL ITO SOL-GEL FILMS

3.1 Effect of Calcination Temperature on Structural, Electrical, Optical and Chemical Properties of 4-layered ITO thin films

3.1.1 XRD Analyses

Figure 3.1 shows the XRD diffractograms of 4-layered plain ITO thin films calcined at different temperatures. The films calcined at 300 °C were amorphous. After calcinations at 400 °C and higher temperatures, the films showed transformation from an amorphous state to a polycrystalline cubic bixbyite In_2O_3 structure (JCPDS card no: 06-0416). No other phases corresponding to Sn compounds were detected, suggesting that the dopant Sn atoms coordinate within In_2O_3 . Moreover, it was observed that the position of diffraction peaks shifts slightly to lower 2θ values relative to peak positions of pure In_2O_3 . This difference is also an indication of Sn doping into In_2O_3 lattice changing the position of diffraction peaks. For this set, when higher calcination temperatures were employed, the crystallinity of the films was improved.

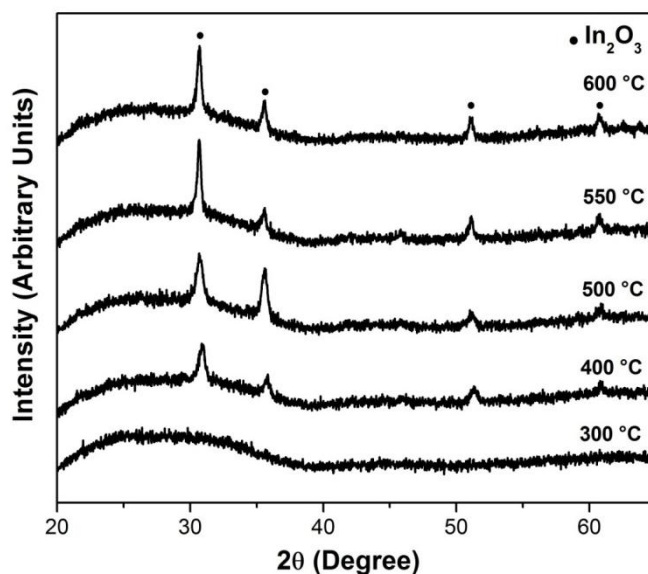


Figure 3.1 XRD diffractogram of 4-layered ITO thin films calcined at different temperatures (for 50 min).

3.1.2 Optical Properties of ITO Films

Figure 3.2 shows the optical transmission spectra of 4-layered ITO thin films that are calcined at different temperatures. For the films calcined at relatively lower temperatures, as for 200 and 300 °C calcined samples, the transmittance values at 550 nm were around 80 – 90 %. For well crystallized films calcined at higher temperatures, such as 550 or 600 °C, these transmittance values are typically in the range of 90 – 95 %. For the thin films formed at relatively lower calcination temperatures, such as 200 or 300 °C, a gradual decrease in the transparency is observed with decreasing wavelength around the UV region (wavelengths smaller than 400 nm). On the other hand, this change is much steeper for the thin films calcined at temperatures higher than 400 °C. In addition, after calcination (200 , 300 °C), ITO thin films turned to black, suggesting that some carbon related organic residuals still exist in the films and degrade the optical properties. Therefore, to obtain ITO thin films with high transparency, calcination temperature should be in

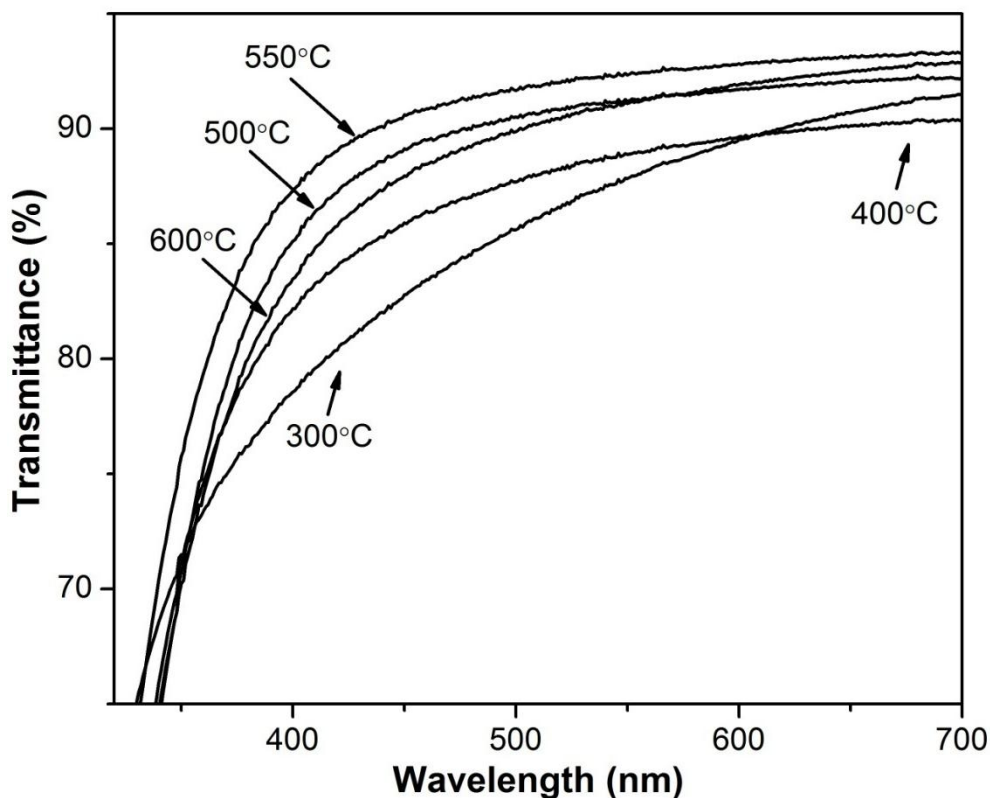


Figure 3.2 Optical transmittance spectra of 4-layered ITO thin films calcined at different temperatures.

the range of 400 to 600 °C. The residual organic groups from the solvents present in ITO thin films at relatively lower calcination temperatures cause absorption in the visible range. As the calcination temperature increased further to 400 °C, transparency is increased due to elimination of these residual organics, which promotes the formation of ITO crystals. These results are consistent with the XRD patterns in Figure 3.1 suggesting the onset of crystallization at 400 °C. The improvement in optical transmittance at higher calcination temperatures can be attributed to the increase of structural homogeneity and crystallinity [18]. The absorption event occurring below 350 nm is most likely caused by the electron excitation from valance band to conduction band, corresponding to energy quanta comparable with the band gap of tin-doped indium oxide (3.5 – 4.3 eV). As the calcination temperature is increased, there is also a decrease in transmission values

close to UV-range, i.e. below 350 nm. This phenomenon can be expressed by an increase in the steepness near the band edge absorption, consistent with the improved crystallinity.

3.1.3 Electrical Properties and Surface Chemistry

Figure 3.3 shows the effect of calcination temperature on the sheet resistance of ITO thin films. The sheet resistance of ITO thin films reaches a minimum value for a calcination temperature of 550 °C. It is well known that by increasing the calcination temperature (in the range of 300 – 500 °C), the sheet resistance of ITO thin films

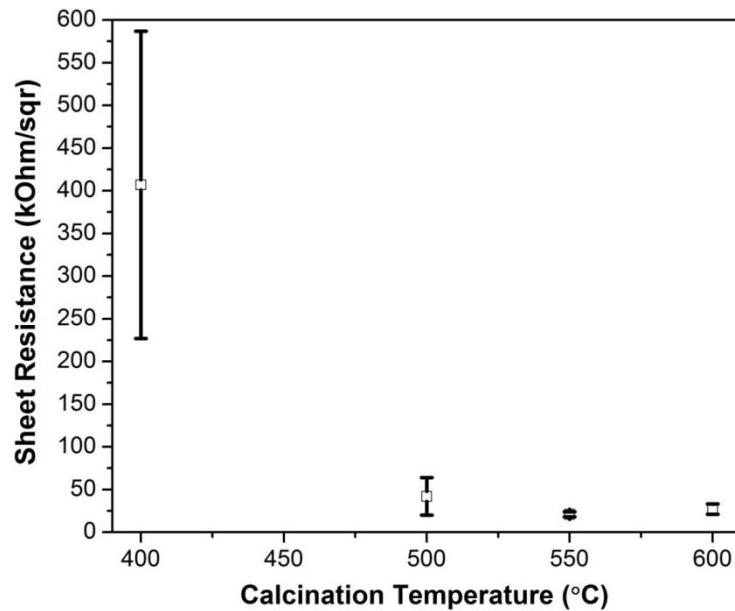


Figure 3.3 Sheet resistance with standard deviations of 4-layered ITO thin films prepared from plain ITO sols as a function of calcination temperature.

decreases due to increased carrier concentration and also due to enhanced crystal growth and improvement in crystallinity. For a microstructure with large crystals, electron-grain boundary scattering decreases, which leads to higher carrier mobility and higher electrical conductivity. On the other hand, with increasing calcination temperature beyond 550 °C, the sheet resistance increases slightly. This might be due to diffusion of impurity ions from the SLS glass substrate into the ITO thin films. Even though the crystallinity of films was improved by calcination at higher temperatures, a calcination process performed above 550 °C is expected to deteriorate the electrical conductivity, due to ion (Na^+ , Ca^{2+} , etc.) exchange from underlying glass substrates. The calcination temperature has been optimized as 550 °C. Calcination temperatures higher than 550 °C slightly increase the sheet resistance of ITO thin films. This observation has also been reported by various authors in the literature as discussed in *Section 1.6.1* of Chapter 1. High temperature calcination increases the diffusion kinetics of high mobile alkali ions in the glass substrate.

Figure 3.4 shows the high resolution regional XPS spectra of ITO thin films calcined at 200, 400 and 600 °C. The concentration of silicon and sodium on the surface of the films increases with the calcination temperature. Na^+ ions diffuse out from the substrate and pass through the film surface degrading the electrical properties of ITO thin films by scattering the charge carriers. On the other hand, significant increase in the Si amount at 600 °C implies that the structural integrity of the film might be lost to some extent due to formation of microcracks.

The change in Si and Na contents (in atomic %) of 4-layered ITO thin film surfaces at different calcination temperatures (200, 400 and 600 °C) are given by the Table 3.1 These results are in agreement with the qualitative results obtained from high resolution XPS spectra of same films (Figure 3.4).

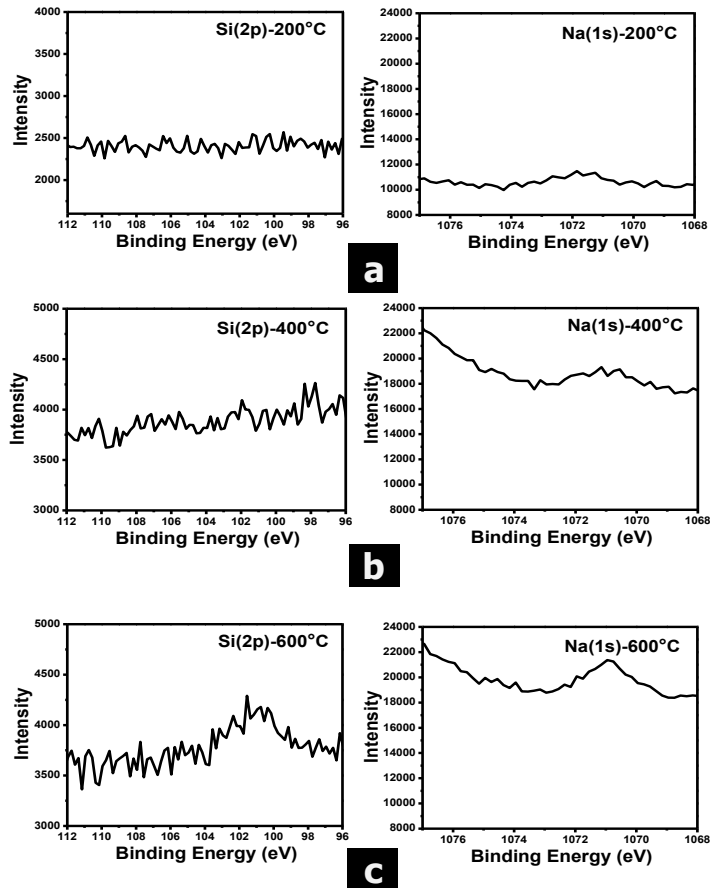


Figure 3.4 High resolution Si(2p) and Na(1s) XPS spectra of 4-layered ITO thin films calcined at (a) 200, (b) 400 and (c) 600 °C.

Table 3.1 Approximate surface Si and Na contents (in atomic %) of 4-layered plain ITO thin films as determined by XPS analyses.

Calcination Temperature	Si (at. %)	Na (at. %)
200 °C	0.4	3.9
400 °C	0.8	10.2
600 °C	1.1	10.5

Na amount on the surface after calcination at 200 °C was found to be 3.9 at %. On the other hand, when the calcination temperature is increased from 400 to 600 °C, Na concentration rises from 10.2 to 10.5 at %. The extent of increase in Na concentration in the range of 400 – 600 °C calcination was obviously low. However, from Figure 3.3, calcination of films at 400 °C and 600 °C results in formation of films with a sheet resistance value of 407 ± 180 and 21 ± 3 kOhm/sqr respectively. Therefore, based on this order of magnitude difference in sheet resistance values, the change in electrical properties of films is not solely controlled by the amount of impurity ions in ITO thin films. It should be noted that the crystallization degree of films calcined at 400 °C is remarkably lower than films calcined at 600 °C (Figure 3.1). The improvement in electrical properties of the films calcined at temperatures higher than 400 °C can be attributed to the enhancement in crystal quality of the films. As a result, although the films contain considerable amount of impurity ions, calcination at 600 °C leads to formation of films with high crystallinity and better electrical performance. Additionally, due to incomplete crystallization at a calcination temperature of 400 °C, resultant films contain a considerable amount of amorphous phase. Therefore, electrical resistance of amorphous regions on the film surface is expected to be higher, which obviously increases the standard deviation values of measured sheet resistance. Films were non-uniform in terms of electrical performance.

3.1.4 Microstructure: Morphological Analyses

Figure 3.5 shows the SEM images of 4-layered ITO thin films calcined at 300 and 600 °C. Both films have a uniform microstructure and compaction efficiency is relatively poor. Pores on the surface of the films calcined at low temperature (300 °C) form a continuous channel (Figure 3.5a). It should be noted that films calcined at 300 °C were amorphous as revealed by XRD analyses (Figure 3.1). It was already mentioned in *Section 3.1.2* that residual organics still persist in the films calcined at 300 °C. Some of the organic compounds present in as-dried films decompose up to 300 °C leading to the formation of a porous network of amorphous ITO phase. On

the other hand, from Figure 3.5b, the degree of densification of ITO thin films slightly increased when the calcination temperature is increased from 300 to 600 °C.

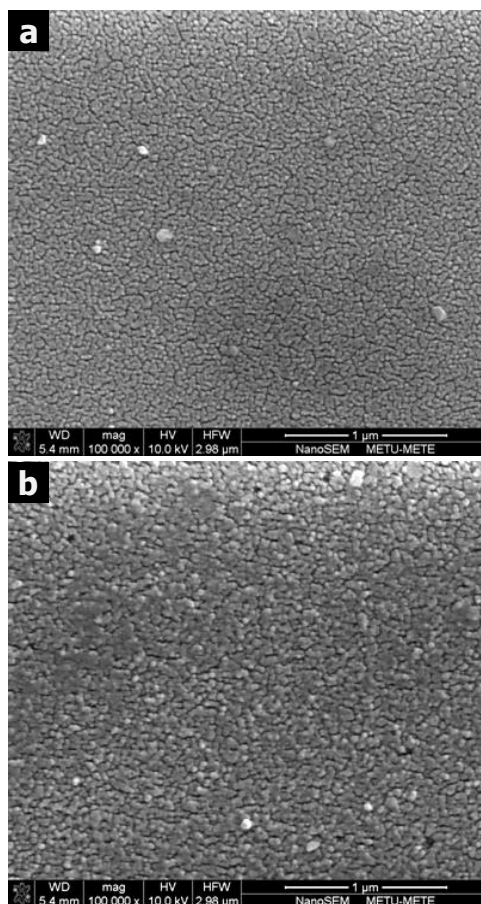


Figure 3.5 Top view SEM images of 4-layered ITO thin film surfaces calcined at (a) 300 and (b) 600 °C.

Once the organics were excluded from the films enabling the formation of ITO crystals, ITO clusters start to grow and coalesce at higher temperatures. However, it should be emphasized that films calcined at high temperature (600 °C) still have considerable amount of porosity.

Both types of films have large white particles on the surface. The amount of these particles is higher for the films calcined at 300 °C. Figure 3.6 shows the energy dispersive x-ray (EDX) spectra of ITO films calcined at 300 °C. The EDX spectra were obtained from different regions on the film surface shown in Figure 3.5a. The SEM image was also included in Figure 3.6 to indicate the regions of the EDX analyses. The spectrum in Figure 3.6a belongs to large white particles on the surface, whereas the general EDX spectrum of the underlying ITO matrix was shown in Figure 3.6b. The unlabeled peak for both spectra at 2.12 keV belongs to $\text{AuM}_{\alpha 1/2}$ and it is coming from the sputtered 7 nm gold film for SEM investigations. It was observed that white particles on the surface contain significant amount of chlorine. The chlorine residues are higher for the films calcined at low temperature (300 °C). It was indicated previously that chlorine impurities in films are detrimental for the electrical properties of ITO thin films (*Section 1.5.1 of Chapter 1*). Additionally, in order to remove these impurities from the films, high temperature calcination is essential. The presence of lower amount of chlorine-based impurity particles on the film surface for the films calcined at 600 °C is due to the decomposition of these particles at higher calcination temperatures. Poor electrical conductivity of films calcined at low temperatures (300 – 500 °C) (Figure 3.3) not only due to poor crystallization, but also due to the presence of chlorine-based impurities from In and Sn precursors.

Regardless of calcination temperature, relatively poor electrical performance of standard/conventional, sol-gel derived ITO thin film is mainly due to the formation of porous microstructure with poor contact between adjacent grains. Synthesis of high density films is essential in order to create more continuous percolation paths on the film surface to increase the mobility of charge carriers.

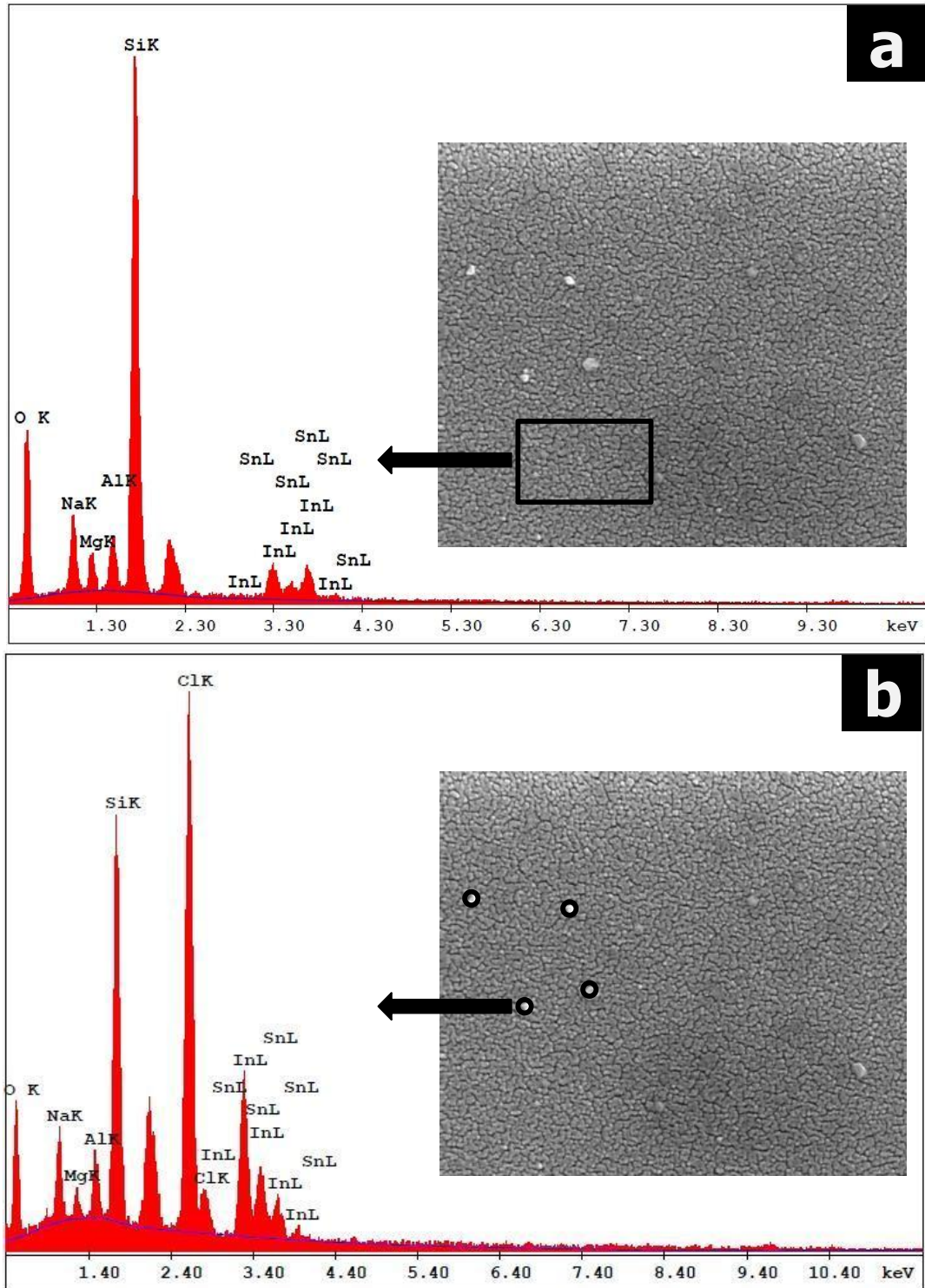


Figure 3.6 Energy dispersive x-ray (EDX) spectra of 4-layered ITO thin films calcined at (a) 300 and (b) 600 °C. Inset reveals the spots where the spectra has been taken.

3.2 Effect of Number of Layers on Optoelectronic Properties and Microstructure of ITO Thin Films

3.2.1 Electrical Properties: Conductivity

The sheet resistance of ITO thin films calcined at 550 °C as a function of the number of deposited layers is shown in Figure 3.7. It can be seen that as the number of coating steps increases from one to ten, the resistance decreases from 86.1 ± 11 kOhm/sqr to a value of 0.9 ± 1 kOhm/sqr respectively. This two orders of magnitude improvement in conductivity of films can be credited to increase in the concentration of carriers due to the formation of thicker films. Additionally, growth of ITO crystals is promoted for multilayered films leading to an enhanced electrical performance. It should also be noted that the standard deviation values of measured sheet resistances decrease considerably by increasing the number of layers. The number of layers can be related to film thickness to a certain extent. A single layer coating operation leads to a film thickness in the order of 47 ± 4 nm, as measured by cross-sectional SEM images (not shown here).

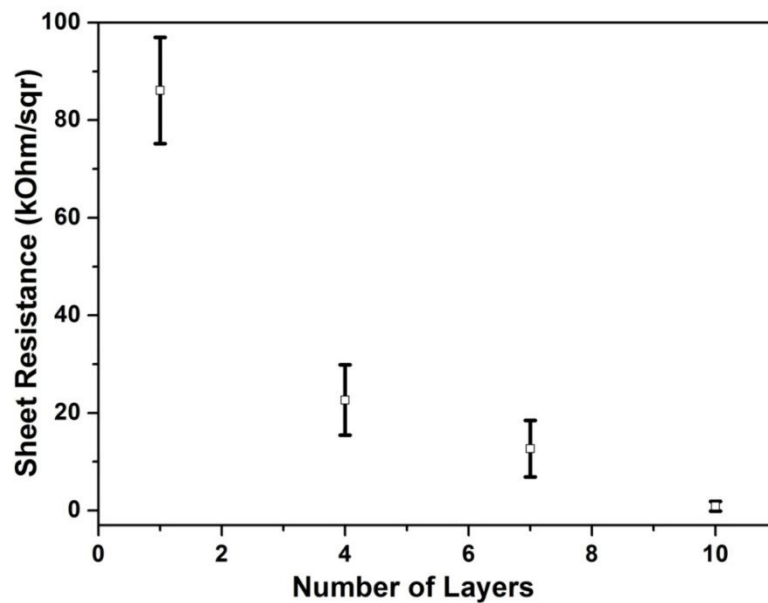


Figure 3.7 Sheet resistance of ITO thin films with standard deviations calcined at 550 °C as a function of number of layers.

3.2.2 Optical Properties: Transmittance

The film thickness also affects the transmittance of ITO thin films. As shown in Figure 3.8, the optical transmittance of the films produced by 1-, 4- and 7-step coating operation(s) are comparable and are in the range of $90\pm 5\%$, and there is only slight reduction in visible light transmittance with increasing film thickness. However, the transmittance remarkably decreases for the films produced by 10 coating operation, reaching to a value of 70%. Lower transmittance observed for multi-layered films is due to the formation of thicker films which lead to an increase in optical absorption.

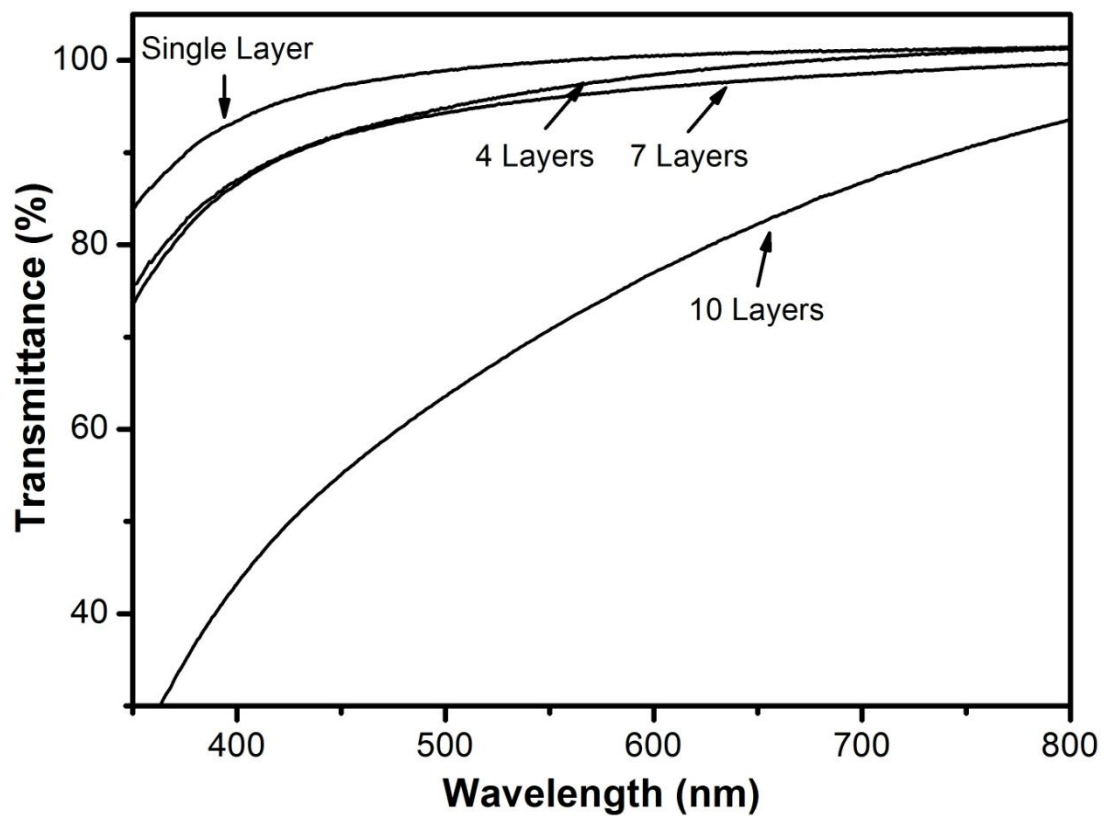


Figure 3.8 Optical transmittance of ITO thin films calcined at $550\text{ }^{\circ}\text{C}$ as a function of number of layers.

3.2.3 Microstructure

Top view SEM images of single-layer and 4-layered ITO thin films calcined at 550 °C are shown in Figure 3.9. It was observed that 4-layered films have lower degree of porosity and thus have higher density than single-layer films. Single-layer films consist of spherical particles attached to each other forming a chain-like entangled morphology leading to the formation of low density films (Figure 3.9a). On the other hand, the surface morphology of ITO thin films changes drastically when the number of coating operations is increased. Based on the surface morphology of 4-layered film (Figure 3.9b), subsequent sol deposition steps fill some of the voids/pores present in the single-layer film in as-dried condition. Consequently, this leads to formation of denser films. The improvement in electrical properties of multi-layered films (Figure 3.7) can also be attributed to the formation of denser films. However, it should be emphasized that even 4-layered films have considerable amount of porosity.

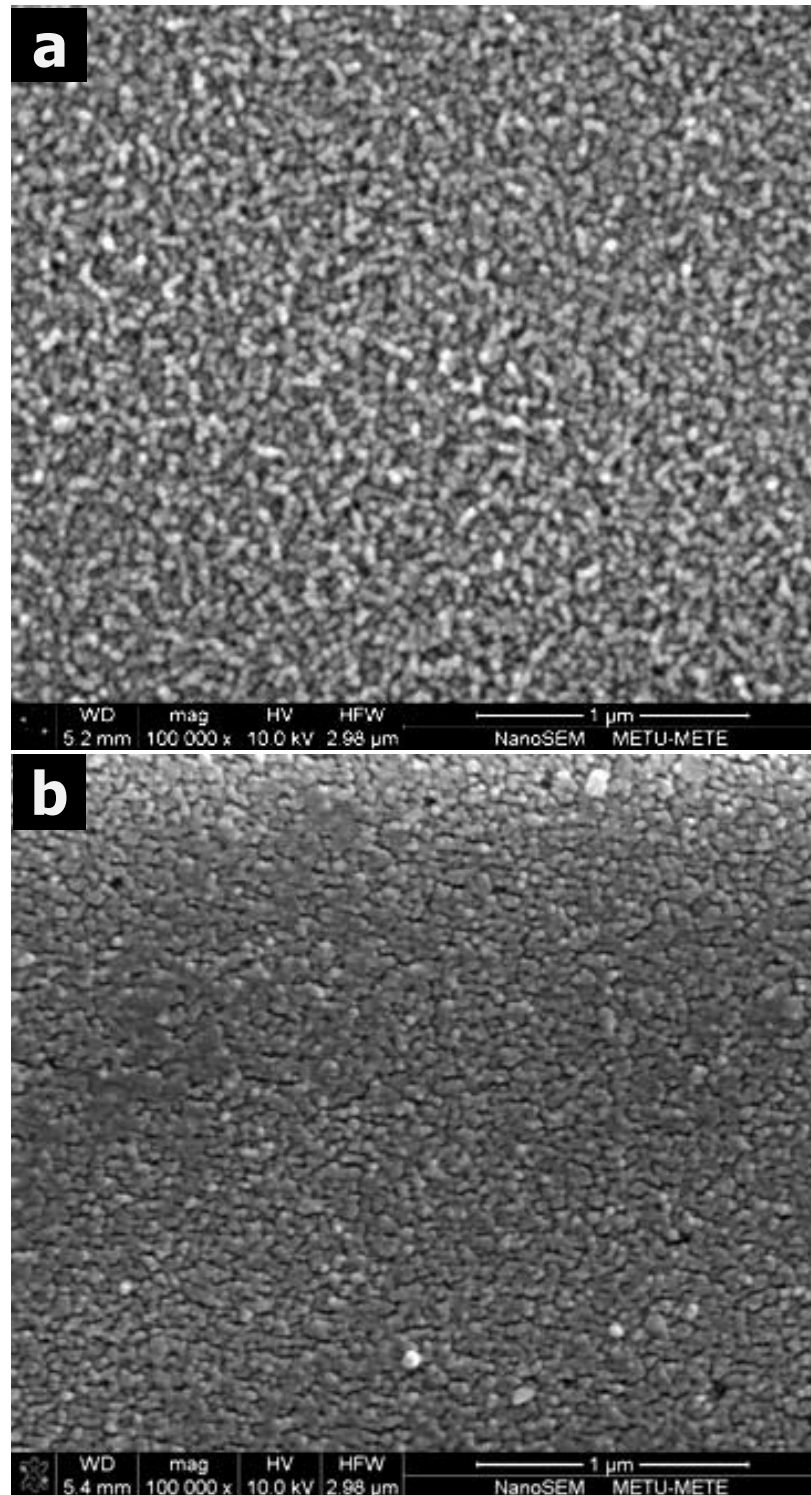


Figure 3.9 Top view SEM images of (a) single-layer and (b) 4-layered ITO thin films calcined at 550 °C.

CHAPTER 4

4. MODIFIED ITO SOL-GEL FILMS: PART I

4.1 Effect of OAD Addition on Structural, Electrical, Optical and Chemical Properties of ITO Thin Films

4.1.1 Phase Analyses and Chemical Structure

Figure 4.1a and 4.1b show the XRD diffractograms of single-layer plain and OAD-modified ITO thin films calcined at different temperatures. OAD-modified film was formed using the *standard* sol formulation corresponding to 0.75 M OAD addition. For both sets of the diffractograms the broad and low intensity hump, expanding in the 2θ range of $20 - 36^\circ$, are from the underlying glass substrate. The films calcined at 300°C were amorphous and higher temperature calcination leads to the formation of a crystalline phase. For both cases, the diffraction peaks match with those for the cubic In_2O_3 (JCPDS card no. 06-0416). For both sets of samples, the crystallization starts somewhere in the range of $300 - 400^\circ\text{C}$ and higher calcination temperature in $300 - 600^\circ\text{C}$ leads to films with higher crystallinity as revealed by relatively more well-defined diffraction peaks. This is especially more pronounced for plain ITO thin films. It should also be noted that OAD-modified films exhibited relatively poorer crystal quality at all calcination temperatures compared to their plain counterparts. Additionally, relatively broader diffraction peaks suggest smaller crystallite size for the modified films. Meanwhile, the relative peak intensities and intensity order are in agreement with the information in the standard JCPDS card, suggesting lack of any preferred orientational crystallographic growth for both types of films.

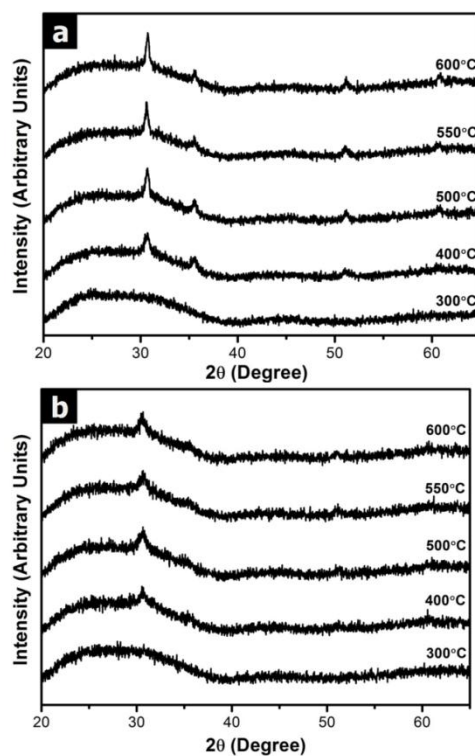


Figure 4.1 XRD diffractograms of (a) plain and (b) *standard* OAD-modified ITO (0.75 M OAD) thin films as a function of calcination (1h, in air) temperature.

The change in ITO phase/crystals with OAD amount in coating sol formulation is represented by the XRD data shown in Figure 4.2. The patterns are for the modified films calcined at 550 °C. An increase in OAD amount results in a progressive decrease in the crystallinity of the films and also in the reduction of the crystallite size. This is revealed by distortion in diffraction peak shapes also accompanied by slight peak broadening.

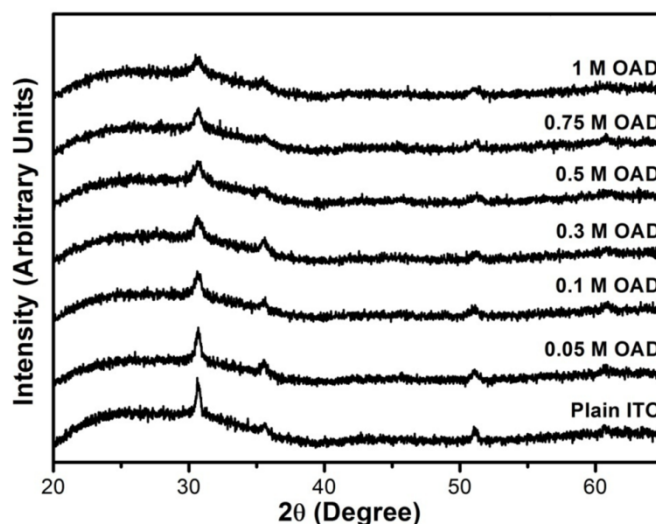


Figure 4.2 XRD diffractograms of OAD-modified ITO thin films with different extent of OAD addition after calcination at 550 °C (1 h, in air).

The XRD findings suggest an amorphous state for both types of ITO thin films in as-prepared condition; however, regardless of the sol formulation, ITO thin films start to crystallize upon calcination at 400 °C or higher temperatures. The thermally induced crystallization of sol-gel derived ITO around 400 °C has been reported in many previous studies conducted using similar sol formulations [77,78,106]. The current study showed that OAD modification evidently changes the crystallization mechanism of the ITO sol-gel films and adversely affects the final crystallization degree achieved after calcination, especially at the lower end of 300 – 600 °C. Relatively poor crystallinity of OAD-modified films may be due to presence of substantial amount of organics, which may still persist at around thermal decomposition range, which is comparable with crystallization temperature (300 – 400 °C) range observed in this study. High amount of organics may hamper inorganic network formation limiting the condensation of hydrated and/or complexed species of In and Sn, as well as subsequent crystallization. The crystallization most likely initiates once the organic compounds in the films are pyrolyzed and completely excluded from the condensing gel. Similarly, poor crystallization efficiency has been reported for the sol-gel derived ITO films formed using PEG- [78] and MPTS/PVP [61] modified ITO sol formulations.

Figure 4.3 shows the transmission FTIR spectra for plain and the *standard* OAD-modified ITO (0.75 M OAD) thin films dried at 100 °C for 10 min. The higher wavenumber (4000 – 1800 cm^{-1}) portion of the spectra revealing only a broad absorption (3670 – 2660 cm^{-1}) for absorbed water has been omitted to clearly show the details of spectra in the presented range of 1800 – 400 cm^{-1} . The two spectra exhibit certain similarities. The main absorption bands positioned at 895 and 763 cm^{-1} were also observed for bare glass (not shown) and assigned for Si–O from glass substrate. The other bands common in both spectra at 1360 and 1430 cm^{-1} are assigned to CH_3 groups of acetylacetone and C=C (at 1525 cm^{-1}) [17]. Both spectra also include a well-defined band assigned for C=O, which appears at 1619 and 1627 cm^{-1} , for plain and OAD-modified film, respectively. The differences between two spectra are marked with the arrows and corresponding wavenumber. Additional absorption bands are detected at 1319 and 811 cm^{-1} for modified films. Moreover, modified films exhibit a weak absorption band located at 668 cm^{-1} , which arise from acetyl acetone ring deformation coupled with In–O stretching [64,107,108]. The plain ITO spectra, on the other hand, exhibit an additional band at 560-490 cm^{-1} attributed to M–O and M–OH vibrations [101,109,110].

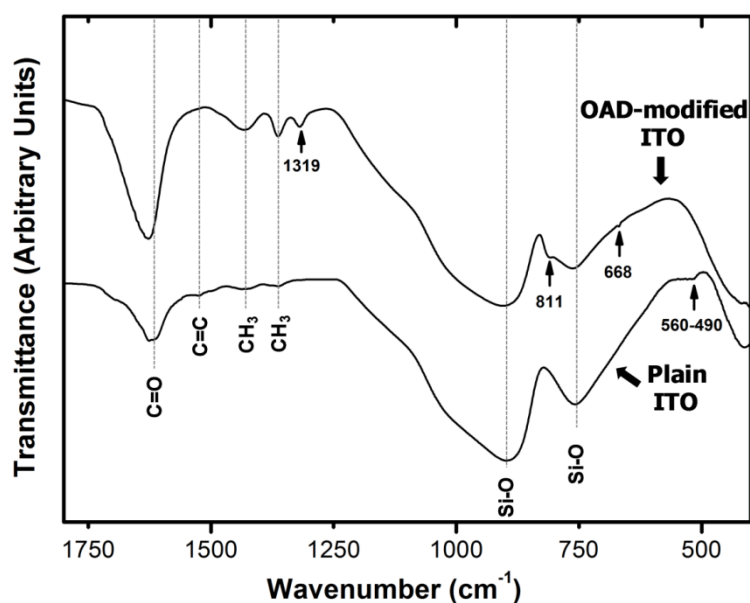


Figure 4.3 FTIR transmittance spectra of plain and *standard* OAD-modified (0.75 M OAD), ITO thin films in as-dried (at 100 °C, 10 min) state.

The spectroscopic investigations (FTIR) point out the chemical differences for plain and OAD-modified ITO sols and more specifically provide insight on the role of acetylacetone and OAD in chemical complexation between these organic molecules and readily dissolved In and Sn ions in the sol. The solvent that has been used in both sol formulations –AcAc– has been also employed as chelating agent for many transition metals and can stabilize metal cations in various ways [76]. It looks like that it also works well in that respect for the ITO sols used in this current study. The complexation of acetylacetone molecules with other chemical species can be easily monitored from spectral investigation based on the absorption associated with the main chemical function carbonyl groups (C=O) in AcAc. The carbonyl group characteristically exhibits absorption around 1700 cm^{-1} assigned to its stretching mode vibration [76,111]. However, association of a metal cation with the carbonyl group results in a positional shift for the characteristic C=O absorption band to lower wavenumbers. For both type of films, the carbonyl stretching absorption bands were found to be at relatively lower wavenumbers; positioned at 1619 and 1627 cm^{-1} for plain and OAD-modified films, respectively. This indicates complexation between metal cations and acetylacetone in both sol systems. The difference in the band positions and absorption band intensities; however, suggest a different chelating mechanism/efficiency for OAD-containing sols. The intensity of stretching of C=O significantly increases in the presence of OAD. This implies association of more C=O groups with metallic ions.

The FTIR findings indicate another important difference between plain and modified sols in terms of chemical bonding. This is revealed by spectral differences in relatively low wavenumber range. The weak absorption band at $560 - 490\text{ cm}^{-1}$ is only observed for plain ITO film assigned to unstabilized metal species, such as M–O and M–OH [64]. The modified films do not exhibit any absorption event in this region. This implies a more effectively condensed inorganic structure for plain ITO thin films. This chemical difference also indicates the possible reason for microstructural/morphological variations for plain and OAD-modified films. Subsequent calcination of films prepared from plain ITO sols results in effective

crystallization and growth of ITO crystallites. However, crystal growth in the modified films in which metal cations is thoroughly stabilized with C=O seems to slowly advance leading to a much smaller crystallite size after calcination. The difference in crystallite size for plain and modified ITO thin films is also emphasized by the XRD data. The relatively broader ITO diffraction peaks for modified films (both in Figure 4.1b and Figure 4.2) point out a relatively smaller crystallite size due to limited crystal growth.

4.1.2 Optical Transmittance and Electrical Conductivity

The change in optical transmittance for both types of ITO thin films as a function of calcination temperature can be realized with the help the UV-Vis spectra shown in Figure 4.4. The OAD-modified thin film was again the *standard* sample (0.75 M OAD). Typically, all films exhibit high transmittance (above 90 % on average) in a wavelength range of 400 – 700 nm. However, for both type of films, increase in the calcination temperature results in higher transparency which is more pronounced in case of OAD-modified films. Meanwhile, it can be said that the addition of OAD

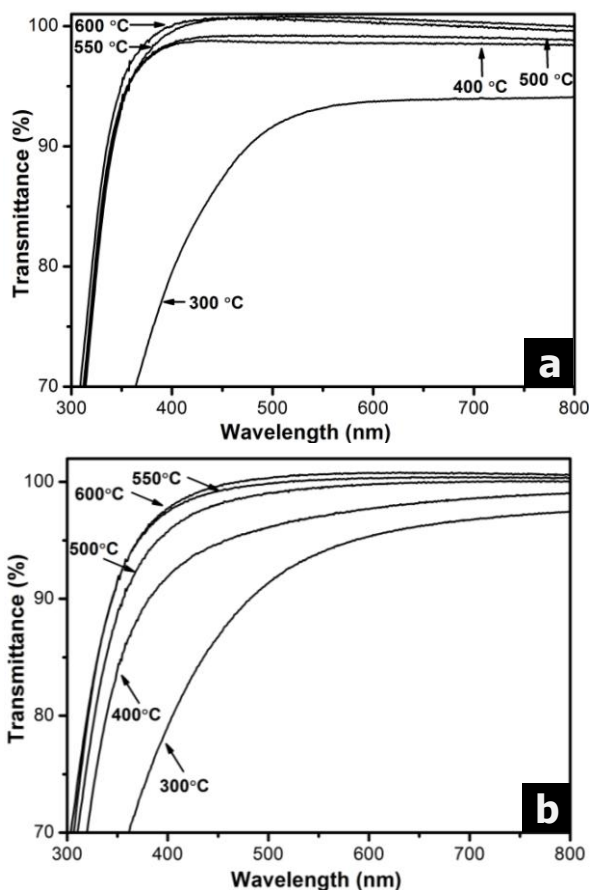


Figure 4.4 Optical transmittance spectra of (a) plain and (b) OAD-modified ITO (0.75 M OAD) thin films as a function of calcination temperature.

slightly decreases (< 2 – 3%) the transparency of ITO thin films. For example, the plain ITO films calcined at same temperature, i.e. 550 °C (in Figure 4.4a) shows an average of 99 % transmittance. On the other hand, ITO thin films modified with 0.75 M OAD exhibit 97 % transmittance in the visible range.

Figure 4.5a and 4.5b show the change in sheet resistance for plain and OAD-modified ITO thin films (0.75 M OAD), respectively, as a function of calcination temperature. The electrical conductivity of the modified film was distinctly higher than that of plain film at all calcination temperatures. However, both types of films exhibit minimum resistance at an optimum calcination temperature of 550 °C.

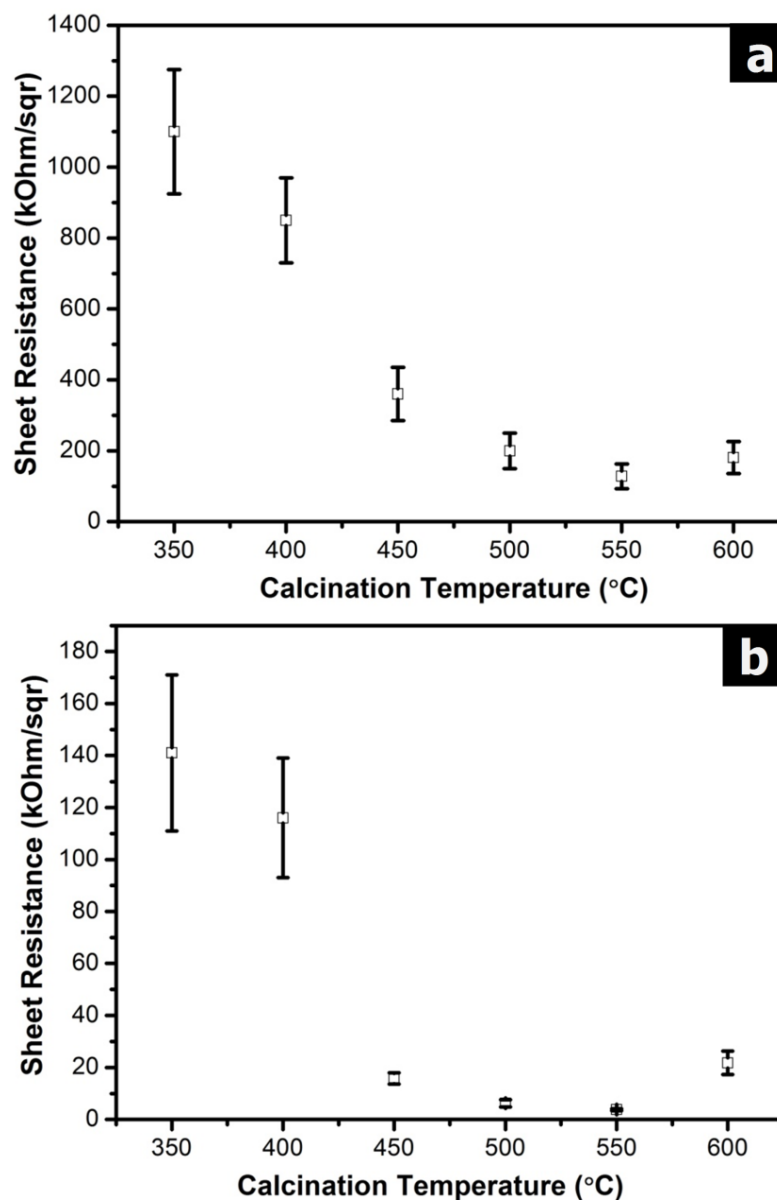


Figure 4.5 Sheet resistance with standard deviations of (a) plain and (b) *standard* OAD-modified ITO (0.75 M OAD) thin films as a function of calcination (1h, in air) temperature.

A calcination treatment at 350 °C, results in a sheet resistance value of 1100±175 and 141±30 kΩ/sqr, for plain and modified film, respectively. However, the resistance of the same films decrease to 128±35 and 3.8±0.4 kΩ/sqr upon calcination at 550 °C. Increasing the calcination temperature to 600 °C, results in a slight increase in the sheet resistance for both types of films. The sheet resistance of the modified film

calcined at the optimum temperature (here 550 °C) was found to be almost two orders of magnitude lower than plain ITO thin film. It should also be noted that increasing the calcination temperature improves the structural and physical homogeneity/uniformity of the films, as indicated by the decrease in standard deviations in the measured sheet resistances.

In regard to optical performance, as a general conclusion, it can be said that higher calcination temperatures improve the transparency of both types of films. The OAD addition leads to a very marginal decrease in transparency. The differences in transmission behavior for amorphous (calcined at 300 °C) and crystalline (calcined at 400 °C or higher temperatures) films clearly show a strong link between crystallinity and optical transmission. It is also worth to mention that both plain and OAD-modified thin films calcined at 300 °C were dark in color indicative of residual organics within the films. Meanwhile, OAD-modified films exhibited lower transparency compared to plain ITO films. Considering the amorphous nature of both films, this observation also supports the presence of higher amount of organics in modified films in as-prepared/as-dried state. The films calcined at higher temperatures (>300 °C) on the other hand were visually transparent and colorless. However, calcination temperature controlled transparency enhancement occurred in a more gradual manner for the modified films as indicated by the UV-Vis data shown in Figure 4a and 4b. Both plain and modified films calcined at 300 °C exhibit absorption extending to a wide wavelength range near the band edge (at around 300 – 350 nm). Calcination treatment at higher temperatures leads to a steeper absorption edge at around 300 nm for both types of films. The sharpening of the fundamental absorption edge of plain ITO thin film occurs only at 400 °C, whereas modified film reaches this state for calcination treatments beyond 500 °C. The calcination temperature-controlled change in transmittance, in fact again signifies the onset of crystallization at temperatures higher than 300 °C, which seems to be somewhat delayed and suppressed for the modified films, as it has been also confirmed by the XRD findings. In that respect, relatively lower optical transmittance of OAD-modified films may arise from poor/inefficient crystallization at 550 °C. Various reports claim formation of more homogeneous and crystalline ITO films upon

calcination at higher temperatures due to lower defect densities which limit/eliminate the photon scattering events, thereby improving optical quality [112].

The change in sheet resistance for the modified ITO thin films as a function of OAD amount can be seen in Figure 4.6. The selected set of samples was calcined at 550 °C. The OAD modification significantly lowers the sheet resistance. In addition, when the OAD addition exceeds a certain level (0.3 M), the standard deviation in measured resistance values reduces drastically, which is most likely due to improvement in physical properties of the resultant films, *i.e.* due to enhancement in film uniformity/homogeneity.

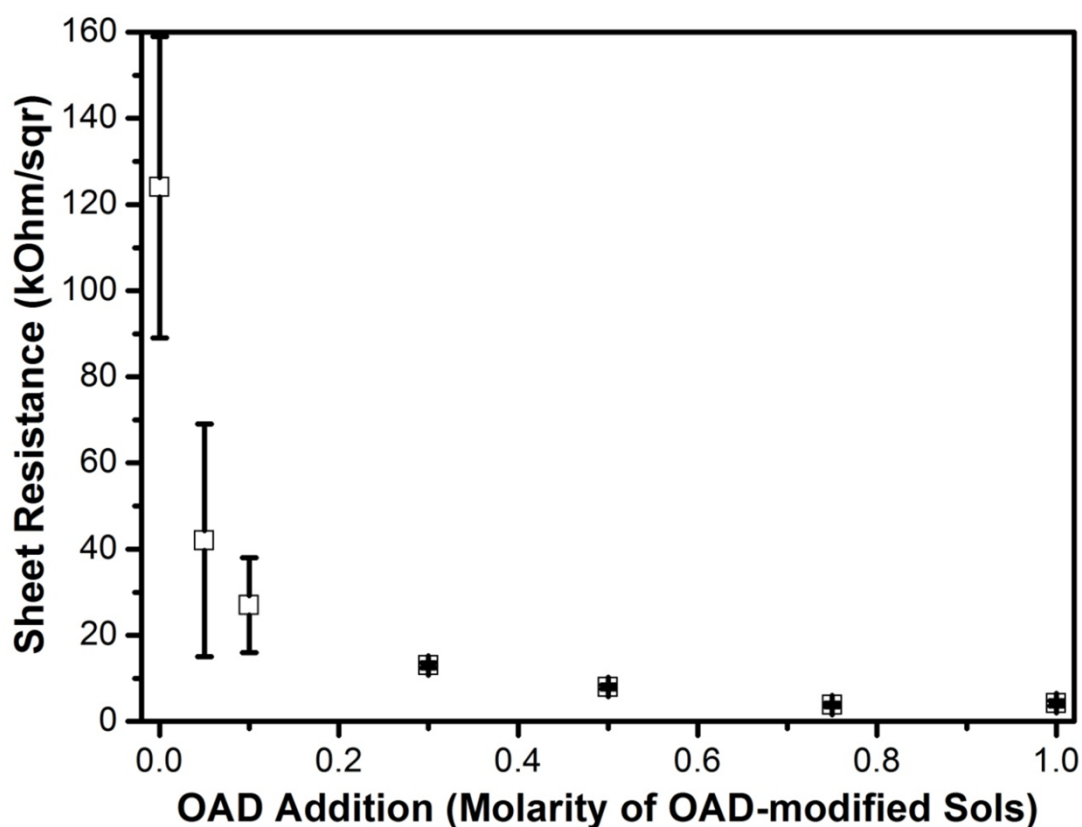


Figure 4.6 Sheet resistance with standard deviations of OAD-modified ITO thin films with different extent of OAD addition after calcination at 550 °C (1 h, in air).

4.1.3 Microstructural Properties: Film Formation, Morphology and Thickness

The cross-sectional and top-view SEM images of plain and OAD-modified ITO (0.75 M OAD) thin films developed by calcination at 550 °C are presented in Figure 4.7. The cross-sectional images are for the films formed on Si wafer using identical coating sols and spin coating parameters. The film thicknesses were comparable and determined as 42 ± 3 and 48 ± 4 nm, for plain (Figure 4.7a) and OAD-modified film (Figure 4.7b), respectively.

Even though the thickness was comparable for both films, the microstructures were different. Figure 4.7c shows the top view SEM image representing the film formation behavior and general appearance of plain ITO thin film (on glass substrate) at low magnification. The film surface was inhomogeneous with distinctly different morphological regions. The OAD-modified film (on glass substrate), on the other hand, exhibited relatively uniform and featureless morphology at millimeter length scale as shown in Figure 4.7d. Figure 4.7e further reveals the microstructural details of the white regions on the plain ITO film surface. The microstructure consists of randomly entangled ITO nanoparticles forming a discontinuous microporous film. The regional energy dispersive x-ray (EDX) spectra (not shown) from that portion on the film revealed an In:Sn atomic ratio of 6.8 – 9.8. Figure 4.7f displays the higher magnification SEM image of gray/black colored regions of the plain ITO thin film surface. It can be seen that surface morphology for this region is relatively denser and larger grains are distributed on film surface. It should be noted that this region contained only trace amount of Sn. The EDX-based chemical composition of the modified film on the other hand was uniform with an In:Sn atomic ratio of 10.3. This value is close to the initial compositional formulation of coatings sol (In:Sn=10 in atomic basis). The microstructural investigations suggest that OAD addition not only enhances the film forming ability of ITO sols, but also affects the chemical characteristics of the resultant films.

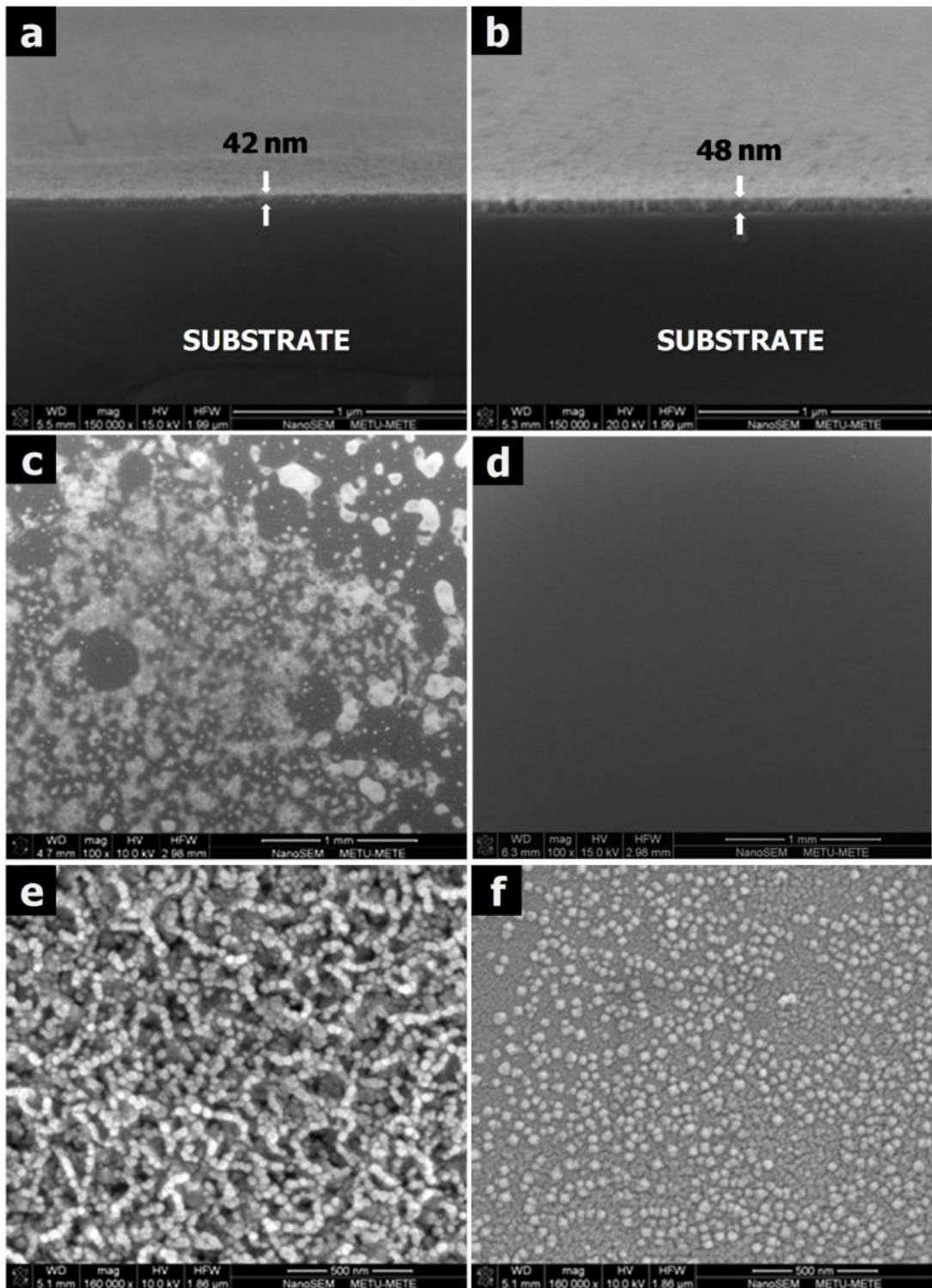


Figure 4.7 Representative cross-section SEM images of (a) plain and (b) *standard* OAD-modified ITO (0.75 M OAD) thin films calcined at 550 °C (1 h, in air). The surface images at low magnification for (c) plain ITO and (d) *standard* OAD-modified ITO (0.75 M OAD) thin films. High magnification images of (e) white regions and (f) gray/black regions on plain ITO surfaces are also indicated.

The higher magnification SEM images of OAD-modified films prepared from coating sols containing different amount of OAD are shown in Figure 4.8a-4.8d. By recalling the typical morphology for plain ITO thin films (shown in Figure 4.7e) it can be said that the OAD addition helps in forming denser films. Moreover, ITO grains seem to have a clustered form composed of very fine particles/crystallites rather than individual spherical particles. The clusters are packed more tightly and firm contacts are established between adjacent clusters in case of films having higher OAD amount (0.75 and 1 M). The SEM results reveal that increasing the amount of OAD in coating solutions improves the microstructure of the ITO thin films.

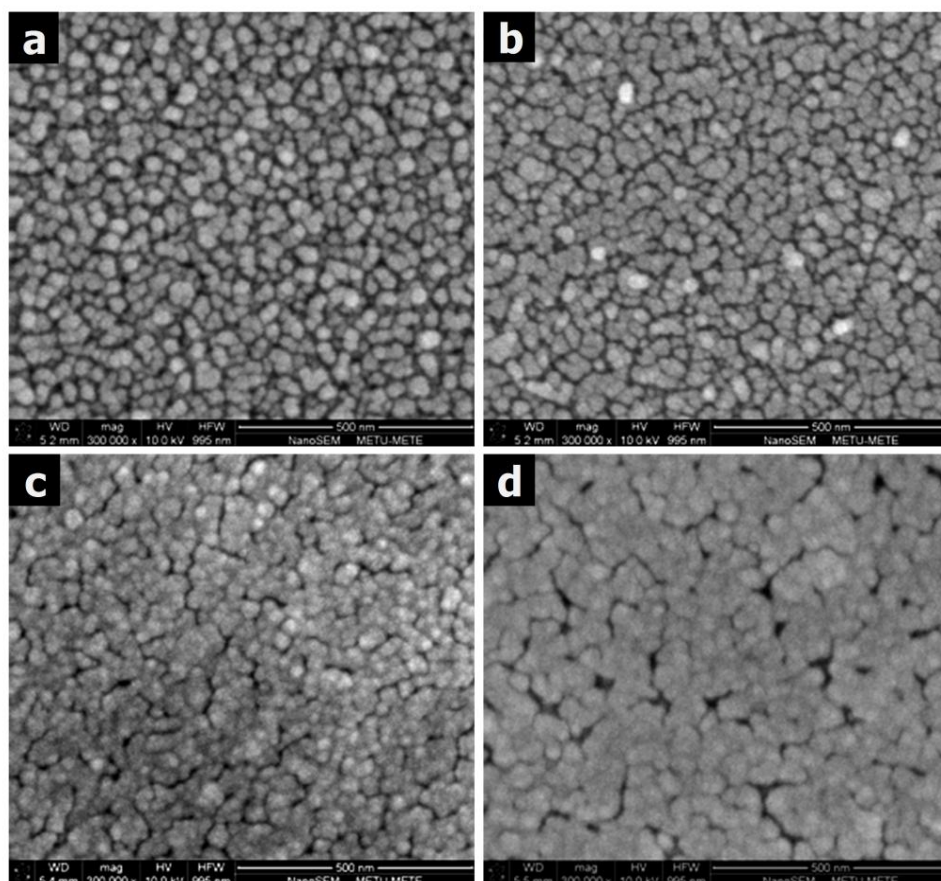


Figure 4.8 Representative top-view SEM images of (a) 0.1, (b) 0.3, (c) 0.75 and (d) 1 M OAD-modified ITO thin films after calcination at 550 °C (1 h, in air).

Accompanying AFM images (Figure 4.9) representative for the SEM images shown in Figure 7e and 8d show the surface properties of plain and OAD-modified films, revealing smoother film coverage for the modified film. The average surface roughness was determined as 8 ± 0.1 nm for plain ITO film and as 4 ± 0.1 nm for 0.75 M OAD-modified film.

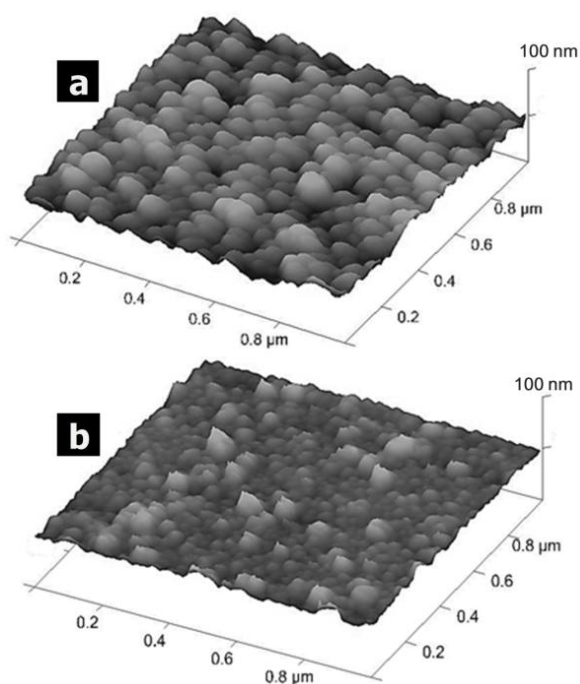


Figure 4.9 AFM images of (a) plain and (b) *standard* OAD-modified ITO (0.75 M OAD) thin films obtained in tapping mode. The average surface roughness values were determined as 8 ± 0.1 nm and 4 ± 0.1 nm, respectively.

Even though OAD incorporation does not seem to be that promising in terms of thermally-induced crystallization and optical properties of ITO thin films, it significantly improves microstructural/morphological properties and the film formation behavior. All these factors are critical for the final electrical conductivity that can be attained. It is worth to mention that the average sheet resistance for plain and OAD-modified films of comparable thicknesses at crystallized state (at 550 °C)

were found as 128 ± 35 and 3.8 ± 0.4 k Ω /sqr, respectively. These values correspond to average bulk resistivities of 0.54 ± 0.12 and 0.02 ± 0.002 Ω cm. The absolute values and standard deviations in the measured conductivities were also improved for OAD-modified films, which can be related to microstructural factors. Formation of more homogenous film coverage at macro level (mm's range) was observed for OAD-modified films (Figure 4.7d). This is attributed to the effective chelation achieved in these modified sols. The relatively high variation in electrical resistivity and chemical composition for plain ITO thin films is also related with the same factor, in other words, inefficient stabilization of cations in the initial coating sol. The chemical variations in the starting sol generate dual-type morphology for plain ITO thin films (Figure 4.7e-f). Differences in regional chemical composition certainly changes the electrical properties locally, therefore causes variations in sheet resistance. Furthermore, both SEM and AFM showed that the OAD-modified films were denser and smoother when compared to plain ITO thin films. Continuous growth of isolated ITO crystals for plain ITO thin films results in development of relatively loose-packed microstructure in nanometer length scale. On the other hand, formation of ITO clusters composed of fine ITO nanoparticles minimizes the porosity for the modified films. Additionally, lower surface roughness values observed for modified films seems to be another microstructural factor for the enhancement of conductivity as also reported by others [60,104,113].

Despite the demand and extensive use of ITO in many optoelectronic applications, enabling economically more feasible processing methods still remains as a challenge. A single step film deposition as described in this work is promising in terms of reducing the elaborative multi-processing tasks, for instance those required in making such films by wet chemical methods in multi-layered form to achieve appreciable electrical conductivity. The bulk resistivity of single layer ITO thin films obtained in this study with optimum amount of OAD modification (0.75 M) was determined to be 0.02 Ω cm exhibiting an optical transmittance of 97 %. Even though the bulk resistivity of commercial grade sputtered ITO thin films obtained is two orders of magnitude lower than the resistivity of the films prepared in this study,

OAD-modified sol-gel thin films are still promising for their use in low-end applications such as antireflective and antistatic coatings on glass.

CHAPTER 5

5. MODIFIED ITO SOL-GEL FILMS: PART II

5.1 Effect of Post Coating Drying Conditions on Performance Properties of OAD-modified ITO Thin Films

Figure 5.1 shows the change in optical transmittance of single-layer OAD-modified films as a function of drying time (10 to 60 min) and temperature (100, 125, 175 and 200 °C). All films exhibit high transmittance (above 96 %) in the visible range of the light spectrum (400 – 700 nm). Regardless of drying temperature, extending the drying process results in a decrease of transmittance of the modified films. It should also be noted that for the same drying time, change in optical transparency of the films do not follow a well-defined trend as a function of drying temperature. This implies that the optical quality of the prepared films strongly depends on the duration of drying instead of drying temperature.

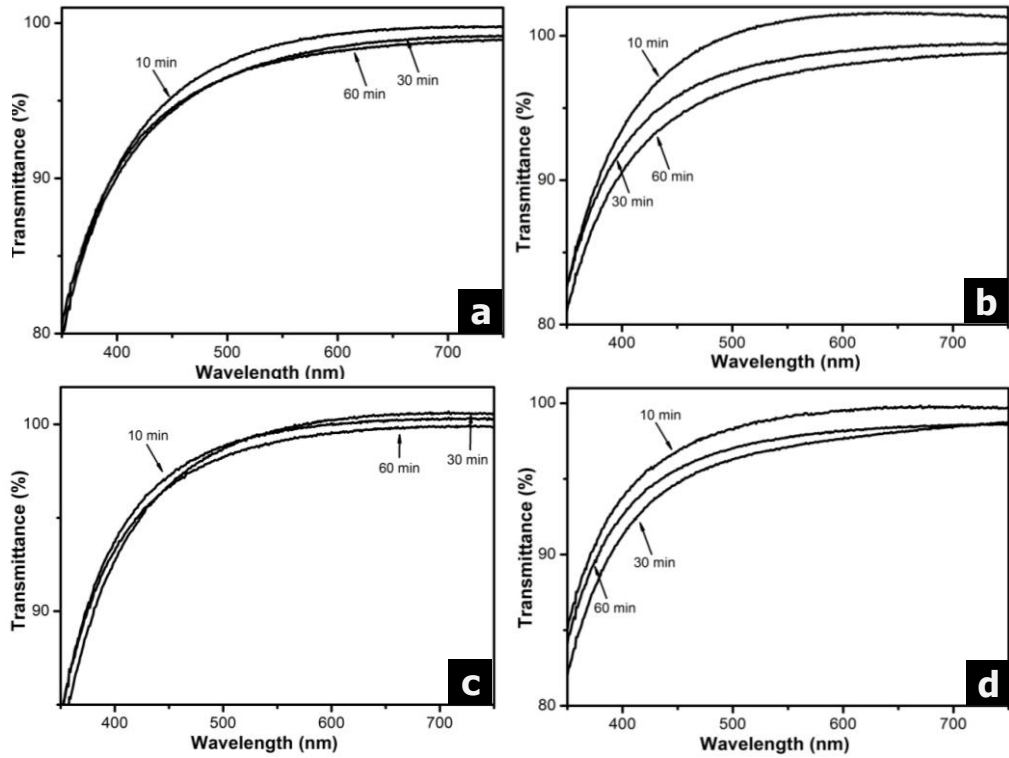


Figure 5.1 Optical transmittance spectra of single-layer ITO thin films dried at (a) 100, (b) 125, (c) 175 and (d) 200 °C for 10, 30, and 60 min.

The effect of drying time (10 to 60 min) and temperature (100, 125, 175 and 200 °C) on sheet resistance of the ITO thin films can be seen from conductivity measurements summarized by the results in Figure 5.2. The films dried at 100 °C for 10 min have the lowest sheet resistance (around 3.8 ± 0.4 k Ω /sqr). Extension of drying process adversely affects the sheet resistance of the films. In addition, the electrical properties of the ITO thin films do not only depend on the drying time, but also got affected by the drying temperature. For the same drying time, sheet resistance of the films increases with the drying temperature. The highest electrical resistivity was measured as 20.5 ± 3.2 k Ω /sqr for the films dried at 200 °C for 60 min. Additionally, increasing the drying temperature increases the standard deviation of the measured values. This observation can be interpreted as the deterioration of the homogeneity of films upon drying at relatively higher temperatures.

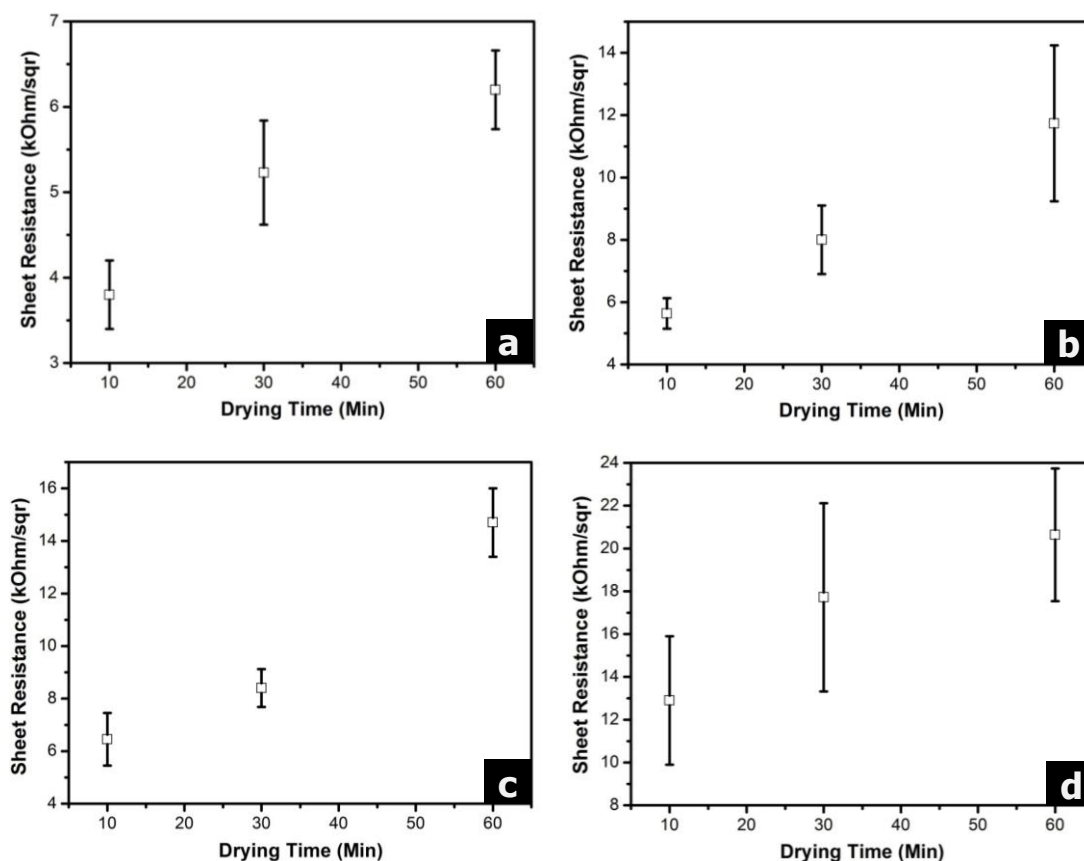


Figure 5.2 Sheet resistance of single-layer modified-ITO thin films dried at (a) 100 , (b) 125, (c) 175 and (d) 200 °C for 10, 30, and 60 min.

5.2 Effect of Post Coating Drying Conditions on Microstructure of OAD-modified ITO Thin Films

Figure 5.3 shows the top-view SEM images of the single-layer thin films dried for 10 min at different drying temperatures of 100, 125, 175 and 200 °C. The surfaces of the films reveal a typical morphology of a sol-gel derived film composed of a nanostructured organization of small crystals with high surface area. As it can be seen from these SEM micrographs, altering the drying temperature does not generate a profound effect on the morphology of the prepared films; the general morphology/microstructure remains same at all temperatures. There are large particles (white colored) distributed evenly on the surface of the films in all cases. In

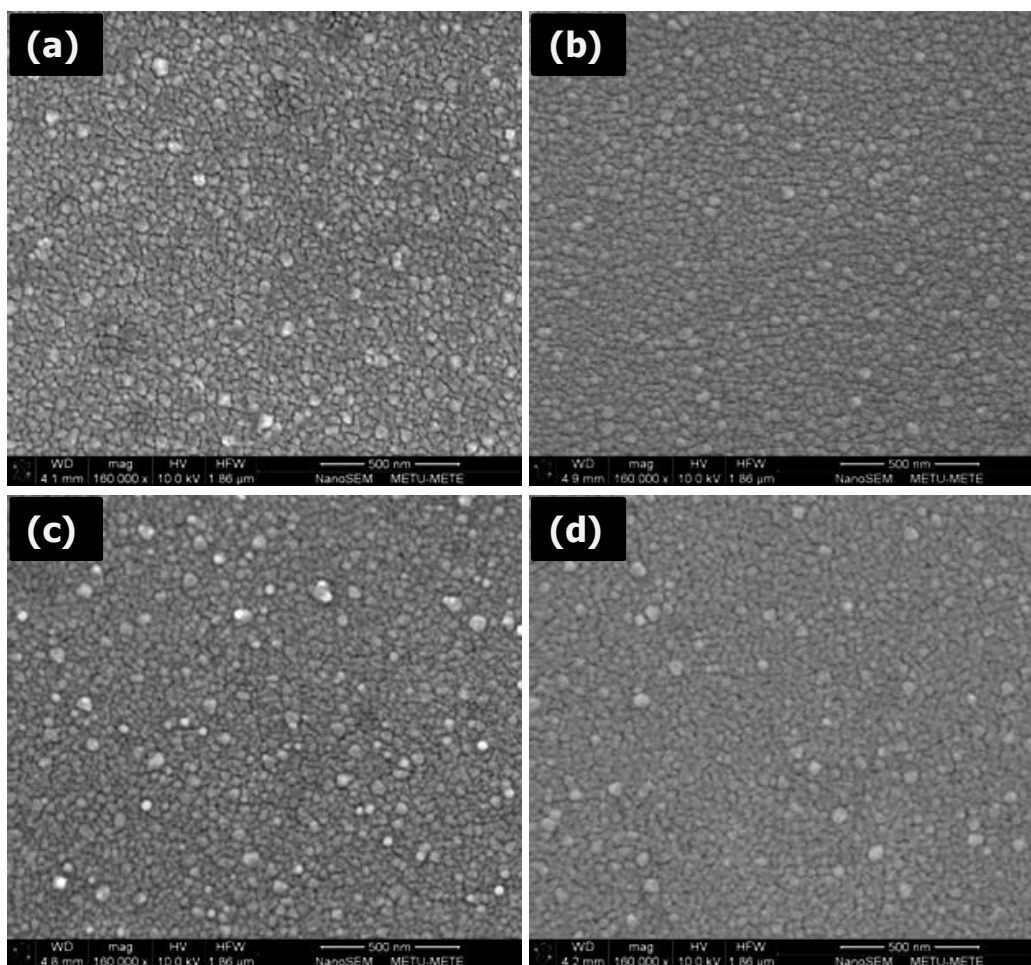


Figure 5.3 Representative SEM images of the surface of the modified-ITO thin films at high magnification (160kx) dried at (a) 100, (b) 125, (c) 175 and (d) 200 °C.

addition, all films exhibit a considerable amount of intergranular porosity leading to poor contact between neighboring ITO crystals/grains.

Figure 5.4 shows the representative SEM images of the single-layer films dried at two different temperatures (100 and 175 °C) for 10 and 60 min. The surface morphologies seem to be unaffected by the change in drying time for the films dried at lower temperatures (100 °C). On the other hand, increasing the duration of drying from 10 to 60 min changes the microstructure of the films dried at 175 °C. From Figure 5.4d, it can be seen that films dried for 60 min have smaller grain size and higher porosity. As previously mentioned, the electrical properties of the films (from

Figure 5.2) dried at higher temperatures/longer times were found to be poor when compared to the films dried at lower temperatures. This can be explained by microstructural changes. The effect of particle size on the electrical resistivity of the ITO films has been reported numerous times in the literature [5,24,29,114]. It is well-known that GB scattering is a significant factor affecting the electrical properties of

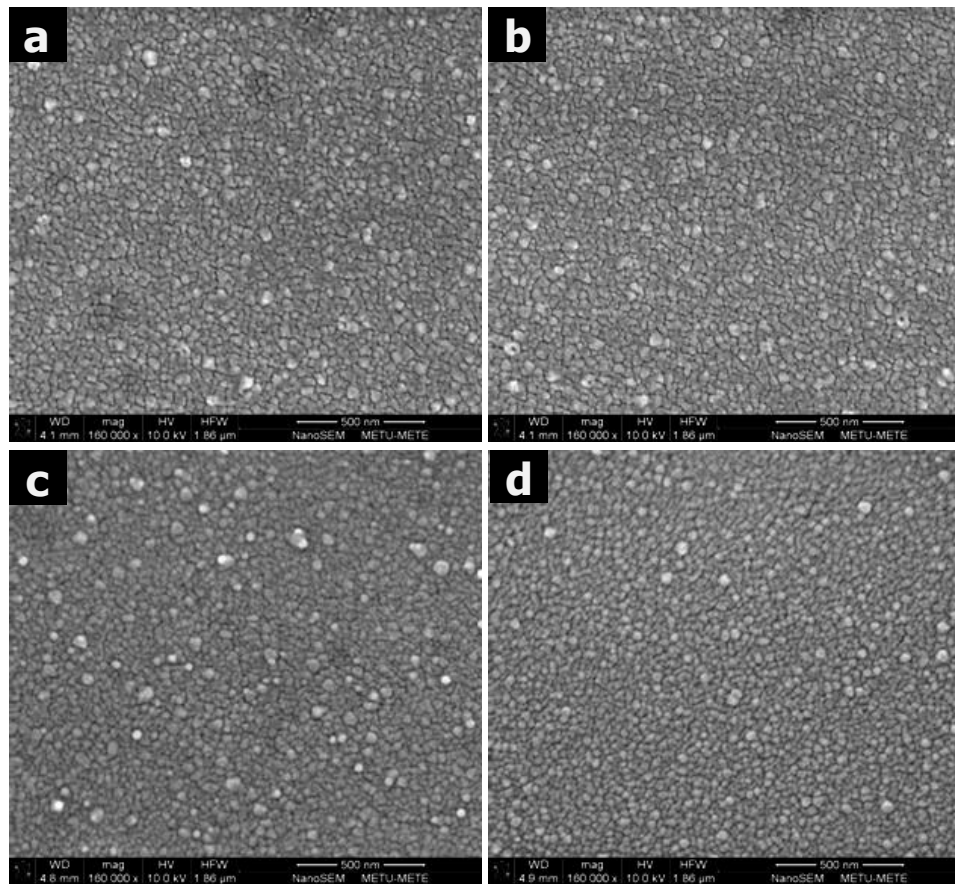


Figure 5.4 Representative SEM images of the surface of the modified-ITO thin films dried at 100 °C for (a) 10 min, (b) 60 min. and at 175 °C for (c) 10 min, (d) 60 min.

thin films. The number of grain boundaries increase as the particle size decreases, which affects the electron mobility. The mean free path of the electron increases due to scattering at GBs. This leads to films with lower conductivities. Moreover, high

amount of porosity also affects the electron mobility negatively by hindering the electron movement. It is thought that high electrical resistance of the films dried at higher temperatures and for longer times is due to combination of these two factors, formation of a more open microstructure and smaller ITO crystals.

Representative low magnification (1000x) SEM images of the films dried at different conditions can be seen from Figure 5.5 providing additional information about the general film characteristics as a function of drying time and temperature. It is worth to mention that the magnification is significantly lower compared to previous SEM images and more representative for general morphology. The films dried at 100 °C for 10 min have a smooth surface (Figure 5.5a) free of any micro cracks and defects. Increasing the drying time to 60 min results in formation of several blisters on the surface (Figure 5.5a). The surface morphology of the films dried at 175 °C for 10 min and 60 min can be seen in Figure 5.5c and Figure 5.5d, respectively. A higher drying temperature leads to the formation of blisters and cracks even for 10 min-dried sample. Increasing the drying time to 60 min at 175 °C results in formation of films having high number of cracks and blisters on the surface. The amount of these defects is significantly increased when compared to films dried at 100 °C. Figure 5.5e and Figure 5.5f show SEM images of single-layer films dried at 200 °C for 10 min and 60 min. It should be noted that even for short drying times, formation of smooth and crack-free films seems to be impossible. Cracks and blisters coexist on the surface of the films. Additionally, the size of the cracks increased significantly. Stoica *et al.* [51] reported that the porosity in sol-gel derived ITO films were due to the presence of volatile species, which were not removed completely before calcination (temperatures at around 550 °C). However, our results indicate formation of such defects in ITO thin films can occur due to drying process as well. Liu *et al.* [59] claimed that film porosity is mainly controlled by the stress build-up and shrinkage of the gel network during drying. Mild drying conditions seemed to be effective in the prevention of these defects. This is somewhat in agreement with our results. As it can be seen from the SEM images (Figure 5.5), blistering seems to occur initially. If excessive stresses develop in the film due to high drying temperatures and longer drying periods, blistered areas start to collapse and form

cracks on the film surface. These might be related to the evolution of gases during removal of organics (acetylacetone and ethanol) readily present in the initial coating sols. In our study, the films were dried in ambient atmosphere previously set to desired drying temperature. Instant heating of the film is quite feasible in terms of process simplicity. However, it can be said that rapid heating causes instant removal of degraded organics from the immature gel network, causing blistering and cracking in the films.

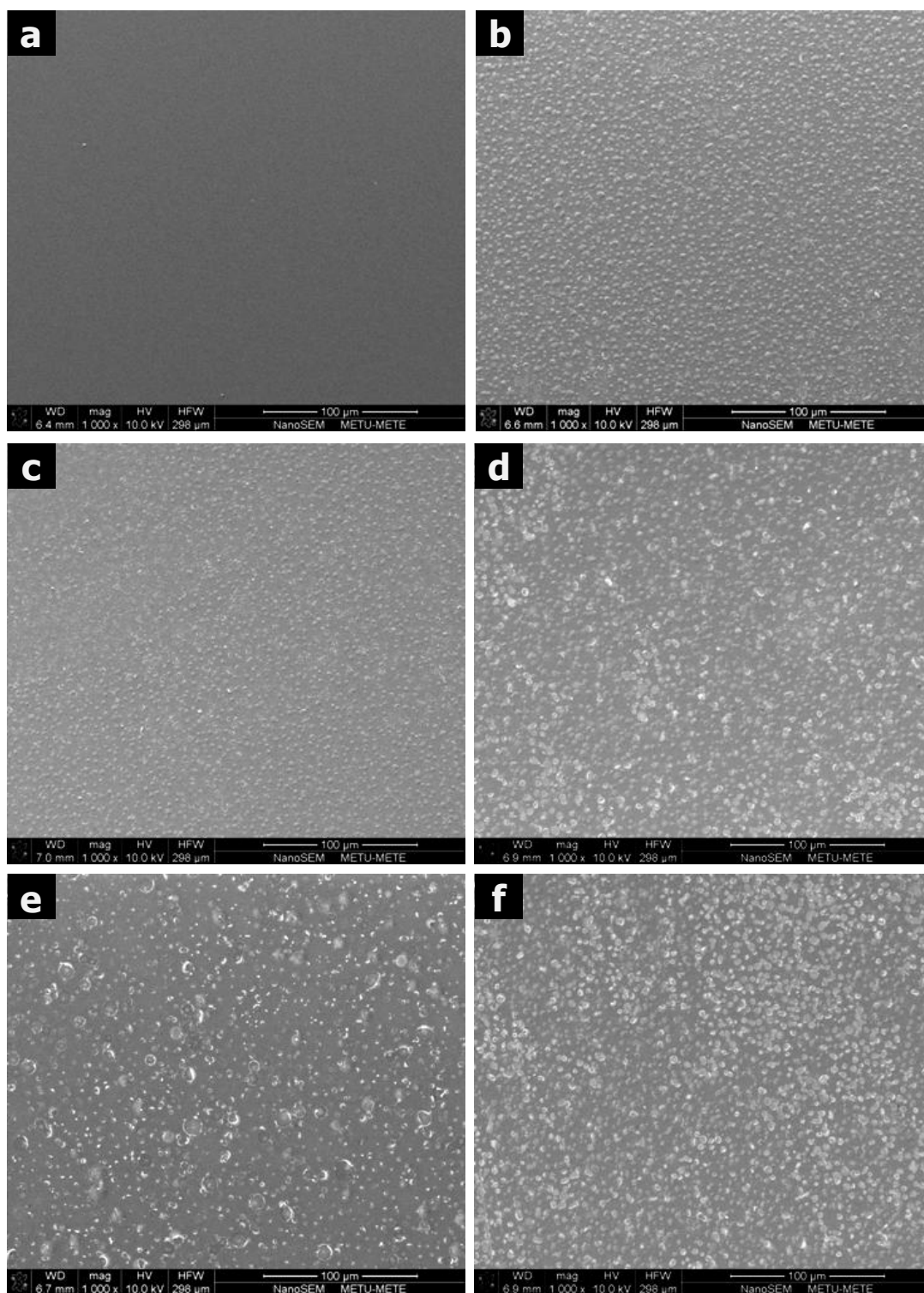


Figure 5.5 Representative top view SEM images of the surface of the single-layer OAD-modified thin films at low magnification (1000x) dried at 100 °C for (a) 10 and (b) 60 min at 175 °C for (c) 10 and (d) 60 min at 200 °C for (d) 10 and, (e) 60 min.

It has been previously reported that thin films differ from bulk form in terms of the amount of stresses developed due to shrinkage of the film on a substrate [115]. Djaoued *et al.* [49] studied the effect of drying time on the sheet resistance of the ITO films prepared by sol-gel. They have found that there is an optimum drying temperature for achieving low sheet resistance values. Even though In and Sn precursors and solvents were different than the chemicals employed in our study, our results also indicate that drying condition has a profound effect in determining the performance properties of ITO thin films prepared by sol-gel methods.

Typically, higher drying temperatures (in the range of 100 - 200 °C) and elongated drying processes (longer than 10 min) both adversely affect the electrical conductivity and increase the sheet resistance of the films due to formation of micro-scaled defects/cracks.

CHAPTER 6

6. CONCLUSIONS

Concluding remarks on processing of *plain/unmodified ITO* thin films

The crystallization of plain ITO thin films was found to initiate at a calcination temperature around 400 °C. The electrical and optical properties of films were improved up to an optimum calcination temperature due to improvements in structural homogeneity, crystallinity and elimination of organic groups from the films.

It was observed that ITO films calcined at 400 °C or higher temperatures contain significant amount of Na impurity ions coming from the glass substrate as revealed by XPS analysis. Presence of Na⁺ in ITO films deteriorates the electrical properties by scattering the charge carriers. However, it is feasible to improve the electrical properties by annealing at higher temperatures due to enhancement in crystallinity.

In addition, regardless of calcination temperature, there were white particles on the surface of ITO films. The amount of these particles was found to be lower for the films calcined at relatively higher temperatures (> 500 °C). Local EDX analysis from the film surface showed that these white particles contain significant amount of chlorine-based impurities. It was concluded that poor electrical conductivity of films calcined at low temperatures (300 – 500 °C) not only related to poor crystallinity and presence of Na⁺ impurities but also arise from the presence of chlorine-based precipitates on film surface from In and Sn precursors.

The improvement in electrical properties of ITO films by increasing the number of coating steps was attributed to the formation of thicker films with higher number of charge carriers. More importantly; the surface morphology of ITO films depends on the number of coating operations performed. Single-layer films have a porous microstructure consisting of spherical particles attached to each other forming a chain-like entangled morphology. On the other hand, subsequent coating operations fill up some of the pores and result in the formation of denser films with improved electrical properties.

Concluding remarks on processing of *OAD-modified* ITO thin films

As a general conclusion, microstructure of the sol-gel derived ITO thin films strongly affects the electrical and optical performance. It has been demonstrated that OAD-modification enhances the electrical properties through certain chemical and microstructural changes for the single-layer ITO films. The crystal quality of ITO was found to be marginally deteriorated and the onset of thermally-induced crystallization was somewhat retarded in the presence of OAD. However, OAD-modification eliminates the chemical variations in coating sol by improving the complexation efficiency between metal cations and organic ligands, therefore enhancing film formation ability, uniformity and surface roughness of the resultant thin films. Additionally, OAD modification also improves the microstructure of single-layer ITO films by enabling formation of more compacted film in nanometer scale.

In addition, post coating drying conditions; namely drying temperature and time was shown to affect the physical properties of OAD-modified films. Typically, higher drying temperatures (in the range of 100 – 200 °C) and elongated drying processes (longer than 10 min) both adversely affect the electrical conductivity and increase the sheet resistance of the films due to formation of micro-scaled defects/cracks. It was also shown that optical quality of the prepared films strongly depends on the duration of drying instead of drying temperature.

Even though the bulk resistivity of commercial grade sputtered ITO films obtained is two orders of magnitude lower than the resistivity of the films prepared in this study, OAD-modified sol-gel films are still promising for use in low-end applications such as antireflective and antistatic coatings on glass.

Future directions

The general scope of sol-gel processing as partially presented in this thesis can be extended in fabricating high performance ITO thin films by wet chemical routes. Deposition of silver-added ITO thin films, for example as mentioned previously in *Section 1.6.1* can be promising for improving electrical conductivity without changing the intrinsic optical transparency of the sol-gel derived ITO host.

One should expect better electrical conductivity for such metal incorporated ITO films and silver nanoparticles or a silver nanowire network can be readily embedded in ITO films by proper modification of the sol formulation. Many different silver-salts and compounds can be easily dissolved in the solvents that have been employed in making ITO films in this current study. The silver ions in ITO sol can be subsequently reduced to metallic form by many different stimuli; including UV or microwave radiations. Therefore, such chemical processing modifications can be implemented/adapted to the experimental deposition techniques offered in the thesis. One critical concern of course is the potential adverse effect of the metallic nano arrangements on optical transmittance, but this can be potentially minimized by controlling size, distribution and alignment of these entities. Even though there are some publications in the recent literature, these technical/scientific points seem to be relatively unexplored for ITO thin films. Such modification can also exclude the need for high temperature calcination treatment, due to higher efficiency in crystallization of amorphous sol-gel ITO host due to presence of well-dispersed metallic local heat centers. This can additionally offer possibilities in fabricating ITO on variety of substrates besides glass and silicon, i.e. on organic substrates with low thermal stability.

REFERENCES

- [1] Exarhos GJ, Zhou XD. Discovery-based design of transparent conducting oxide films. *Thin Solid Films* 2007;515:7025.
- [2] Gordon RG. Criteria for choosing transparent conductors. *MRS Bulletin* 2000;25:52.
- [3] Granqvist CG. Transparent conductors as solar energy materials: a panoramic review. *Solar Energy Materials and Solar Cells* 2007;91:1529.
- [4] Minami T. Transparent conducting oxide semiconductors for transparent electrodes. *Semiconductor Science and Technology* 2005;20:35.
- [5] Granqvist CG, Hultaker A. Transparent and conducting ITO films: new developments and applications. *Thin Solid Films* 2002;411:1-5.
- [6] Livage J. Sol-gel electrochromic coatings and devices: a review. *Solar Energy Materials and Solar Cells* 2001;68:365-381.
- [7] Aegerter MA. Wet-chemical processing of transparent and antiglare conducting ito coating on plastic substrates 2003:81-89.
- [8] Ginley DS, Bright C. Transparent conducting oxides. *MRS Bulletin* 2000;25:15-18.
- [9] Lewis BG, Paine DC. Applications and processing of transparent conducting oxides. *MRS Bulletin* 2000;25:22-27.
- [10] Minami T. Highly transparent and conductive rare earth-doped ZnO thin films prepared by magnetron sputtering. *Thin Solid Films* 2000;366:63-68.
- [11] Shaltout AA, Afify HH, Ali SA. Elucidation of fluorine in SnO₂:F sprayed films by different spectroscopic techniques. *Journal of Electron Spectroscopy and Related Phenomena* 2012.
- [12] Minami T, Takeda Y, Takata S, Kakumu T. Preparation of transparent conducting In₄Sn₃O₁₂ thin films by dc magnetron sputtering. *Thin Solid Films* 1997;309:13-18.

- [13] Minami T, Miyata T, Yamamoto T. Work function of transparent conducting multicomponent oxide thin films prepared by magnetron sputtering. *Surface and Coatings Technology* 1998;108-109:583-587.
- [14] Kawazoe H, Yanagi H, Ueda K, Hosono H. Transparent p-type conducting oxides: design and fabrication of p-n heterojunctions. *MRS Bulletin* 2000;25:28-36.
- [15] Scanlon DO, Walsh A, Watson GW. Understanding the p-type conduction properties of the transparent conducting oxide CuBO_2 : a density functional theory analysis. *Chemistry of Materials* 2009;21:4568-4576.
- [16] Minami T. Present status of transparent conducting oxide thin-film development for indium-tin-oxide (ITO) substitutes. *Thin Solid Films* 2008;516:5822.
- [17] Minami T. New n-type. *MRS Bulletin* 2000;25:38.
- [18] Kim SS, Choi SY, Park CG, Jin HW. Transparent conductive ITO thin films through the sol-gel process using metal salts. *Thin Solid Films* 1999;347:155.
- [19] Lowe AC. Flexible flat panel displays wiley-sid series in display technology. John Wiley and Sons; 2005.
- [20] Freeman AJ, Poepelmeier KR, Mason TO, Chang RPH, Marks TJ. Chemical and thin-film strategies for new transparent conducting oxides. *MRS Bulletin* 2000;25:45-51.
- [21] Burstein E. Anomalous optical absorption limit in InSb. *Physical Review* 1954;93:632.
- [22] Coutts TJ, Young DL, Li X. Characterization of transparent conducting oxides. *MRS Bulletin* 2000;25:58.
- [23] Zhang DH, Ma HL. Scattering mechanisms of charge carriers in transparent conducting oxide films. *Applied Physics A: Materials Science & Processing* 1996;62:487.
- [24] Ramanan SR. Dip coated ITO thin-films through sol-gel process using metal salts. *Thin Solid Films* 2001;389:207.
- [25] Takahashi Y, Okada S, Tahar RBH, Nakano K, Ban T, Ohya Y. Dip-coating of ito films. *Journal of Non-Crystalline Solids* 1997;218:129.
- [26] Dahoudi NA, Aegerter MA. Comparative study of transparent conductive $\text{In}_2\text{O}_3:\text{Sn}$ (ITO) coatings made using a sol and a nanoparticle suspension. *Thin Solid Films* 2006;502:193.

- [27] Frank G, Köstlin H. Electrical properties and defect model of tin-doped indium oxide layers. *Applied Physics A: Materials Science & Processing* 1982;27:197.
- [28] Warschkow O, Ellis DE, Gonzales GB, Mason TO. Defect structures of tin-doped indium oxide. *Journal of American Ceramic Society* 2003;706:1700.
- [29] Tahar RBH, Ban T, Ohya Y, Takahashi Y. Tin doped indium oxide thin films: electrical properties. *Journal of Applied Physics* 1998;83:2631.
- [30] Tomonaga H. Indium–tin oxide coatings via chemical solution deposition. *Thin Solid Films* 2001;392:243.
- [31] Meng L-jian, dos Santos M. Properties of indium tin oxide films prepared by rf reactive magnetron sputtering at different substrate temperature. *Thin Solid Films* 1998;322:56-62.
- [32] Kim H, Piqué A, Horwitz JS, Mattoussi H, Murata H, Kafafi ZH, Chrisey DB. Indium tin oxide thin films for organic light-emitting devices. *Applied Physics Letters* 1999;74:3444.
- [33] Sawada Y, Kobayashi C, Seki S, Funakubo H. Highly-conducting indium – tin-oxide transparent films fabricated by spray cvd using ethanol solution of indium (iii) chloride and tin (ii) chloride. *Thin Solid Films* 2002;409:46-50.
- [34] George J, Menon C. Electrical and optical properties of electron beam evaporated ITO thin films. *Surface and Coatings Technology* 2000;132:45.
- [35] Rozati SM, Ganj T. Transparent conductive sn-doped indium oxide thin films deposited by spray pyrolysis technique. *Renewable Energy* 2004;29:1671-1676.
- [36] Legnani C, Lima S, Oliveira H, Quirino W, Machado R, Santos R, Davolos M, Achete C, Cremona M. Indium tin oxide films prepared via wet chemical route. *Thin Solid Films* 2007;516:193.
- [37] Gao G. *Nanostructures & nanomaterials: synthesis, properties & applications*. 1st ed. London: Imperial College Press; 2004.
- [38] Kulkarni AK, Schulz KH, Lim TS, Khan M. Dependence of the sheet resistance of indium-tin-oxide thin films on grain size and grain orientation determined from x-ray diffraction techniques. *Thin Solid Films* 1999;345:273.
- [39] Cho H, Yun YH. Characterization of indium tin oxide (ITO) thin films prepared by a sol – gel spin coating process. *Ceramics International* 2011;37:615.

- [40] Pulker HK. Coatings on glass. 2nd ed. Amsterdam: Elsevier; 1999.
- [41] Ohring M. Materials science of thin films: deposition and structure. 2nd ed. Academic Press; 1991.
- [42] Patil SP. Versatility of chemical spray pyrolysis technique. *Materials Chemistry and Physics* 1999;59:185.
- [43] Mooney JB, Radding SB. Processing. *Annual Review of Materials Research* 1982;12:81-101.
- [44] Klein LC. For thin films, edited by Klein LC. 1st ed. William Andrew; 1989.
- [45] Brinker CJ, Scherer GW. Sol-gel science: the physics and chemistry of sol-gel processing. 1st ed. San Diego: Elsevier; 1990.
- [46] Schwartz RW, Schneller T, Waser R. Chemical solution deposition of electronic oxide films. *Comptes Rendus Chimie* 2004;7:433.
- [47] Mitzi DB. Solution processing of inorganic materials. John Wiley & Sons; 2008.
- [48] Aegerter MA, Puetz J, Gasparro G, Dahoudi NA. Versatile wet deposition techniques for functional oxide coatings. *Optical Materials* 2004;26:155.
- [49] Djaoued Y, Phong VH, Badilescu S, Ashrit PV, Girouard FE, Truong VV. Sol-gel-prepared ito films for electrochromic systems. *Thin Solid Films* 1997;293:108.
- [50] Toki M, Aizawa M. Sol-gel formation of ITO thin film from a sol including ITO powder. *Journal of Sol-Gel Science and Technology* 1997;8:717-720.
- [51] Stoica TF, Teodorescu VS, Blanchin MG, Stoica TA, Gartner M, Losurdo M, Zaharescu M. Morphology, structure and optical properties of sol-gel ITO thin films. *Materials Science* 2003;101:222-226.
- [52] Kololuoma T, Johansson L-S, Maaninen A, Campbell JM, Rantala JT. Effect of the h₂ annealing on the electrical properties of In₂O₃-SnO₂ thin films. *Journal of Sol-Gel Science and Technology* 2004;32:179.
- [53] Stoica FT, Stoica TA, Vanca V, Lakatos E, Zaharescu M. Colloidal sol-gel ITO films on tube grown silicon. *Thin Solid Films* 1999;348:273.
- [54] Alam MJ, Cameron DC. Characterization of transparent conductive ITO thin films deposited on titanium dioxide film by a sol-gel process. *Surface and Coatings Technology* 2001;142-144:776.

- [55] Alam MJ, Cameron DC. Optical and electrical properties of transparent conductive ito thin films deposited by sol-gel. *Thin Solid Films* 2000;377:455.
- [56] Biswas PK, Ortner K, Korder S. Study of sol-gel-derived high tin content indium tin oxide (ITO) films on silica-coated soda lime silica glass. *Materials Letters* 2004;58:1540.
- [57] Daoudi K, Sandu CS, Moadhen A, Ghica C, Canut B, Teodorescu VS, Blanchin MG, Roger JA, Oueslati M, Bessais B. ITO spin-coated porous silicon structures. *Materials Science and Engineering B* 2003;101:262.
- [58] Beaurain A, Dufour C, Koncar V, Capoen B, Bouazaoui M. Effects of annealing temperature and heat-treatment duration on electrical properties of sol-gel derived indium-tin-oxide thin films. *Thin Solid Films* 2008;516:4102.
- [59] Liu J, Wu D, Zhang N, Wang Y. Effect of surfactants on the structure and photoelectric properties of ITO films by sol-gel method. *Rare Metals* 2010;29:143.
- [60] Gan Y, Liu J, Zeng S. Transparent conductive indium tin oxide film fabricated by dip-coating technique from colloid precursor. *Surface and Coatings Technology* 2006;201:25 - 29.
- [61] Wu D, Liu J, Wang Y. Enhancing indium tin oxide (ITO) thin film adhesiveness using the coupling agent silane. *Applied Surface Science* 2010;256:2934-2938.
- [62] Biswas PK, De A, Pramanik NC, Chakraborty PK, Ortner K, Hock V, Korder S. Effects of tin on ir reflectivity, thermal emissivity, hall mobility and plasma wavelength of sol-gel indium tin oxide films on glass. *Materials Letters* 2003;57:2326.
- [63] Ting C-C, Cheng W-L, Lin G-C. Structural and opto-electrical properties of the tin-doped indium oxide thin films fabricated by the wet chemical method with different indium starting materials. *Thin Solid Films* 2011;519:4286.
- [64] Epifani M, Raül D, Arbiol J, Siciliano P, Morante JR. Solution synthesis of thin films in the SnO₂-In₂O₃ system: a case study of the mixing of sol-gel and metal-organic solution processes. *Chemistry of Materials* 2006;18:840.
- [65] Hong SJ, Kim YH, Han JI. Development of ultrafine indium tin oxide (ITO) nanoparticle for ink-jet printing by low-temperature synthetic method. *IEEE Transactions on Nanotechnology* 2008;7:172.
- [66] Ederth J, Hultaker A, Heszler P, Niklasson AG, Granqvist CG, Van Doorn A, Burgard D. Electrical and optical properties of thin films prepared by spin

coating a dispersion of nano-sized tin-doped indium oxide particles. *Smart Materials and Structures* 2002;11:675.

- [67] Goebbert C, Nonninger R, Aegerter MA, Schmidt H. Wet chemical deposition of ato and ITO coatings using crystalline nanoparticles redispersable in solutions. *Thin Solid Films* 1999;351:79.
- [68] Daoudi K, Sandu CS, Teodorescu VS, Ghica C, Canut B, Blanchin MG, Roger JA, Oueslati M. Rapid thermal annealing procedure for densification of sol-gel indium tin oxide thin films. *Crystal Engineering* 2002;5:187.
- [69] Schwab AP, Lütthge T, Jahn R, Herbig B, Löbmann P. Modified procedure for the sol-gel processing of indium-tin oxide (ITO) films. *Journal of Sol-Gel Science and Technology* 2008;47:68.
- [70] Kuznetsova SA, Malinovskaya TD, Zaitseva ES, Sachkov VI. Indium-tin oxide films obtained from solutions based on acetylacetone. *Russian Journal of Applied Chemistry* 2004;77:1609.
- [71] Mottern ML, Tyholdt F, Ulyashin A, Van Helvoort ATJ, Verweij H, Bredesen R. Textured indium tin oxide thin films by chemical solution deposition and rapid thermal processing. *Thin Solid Films* 2007;515:3918.
- [72] Hammad TM. Effect of annealing on electrical, structural, and optical properties of sol-gel ITO thin films. *Physica Status Solidi A* 2009;206:2128.
- [73] Houg B. Tin doped indium oxide transparent conducting thin films containing silver nanoparticles by sol-gel technique. *Applied Physics Letters* 2005;87:1.
- [74] Li ZH, Ren DY. Fabrication and structure characterization of ITO transparent conducting film by sol-gel technique. *Transactions of Nonferrous Metals Society of China* 2007;17:665.
- [75] Steinbach JF, Freiser H. Acetylacetone. *Analytical Chemistry* 1953;25:881.
- [76] Seco M. Acetylacetone: a versatile ligand. *Journal of Chemical Education* 1989;66:779.
- [77] Nishio K, Sei T, Tsuchiya T. Preparation and electrical properties of ITO thin films by dip-coating process. *Journal of Materials Science* 1996;31:1761.
- [78] Zhang J, Au KH, Zhu ZQ, O'Shea S. Sol-gel preparation of poly(ethylene glycol) doped indium tin oxide thin films for sensing applications. *Optical Materials* 2004;26:47.

- [79] Zhang X, Wu W, Tian T, Man Y, Wang J. Deposition of transparent conductive mesoporous indium tin oxide thin films by a dip coating process. *Materials Research Bulletin* 2008;43:1016.
- [80] Pohl A, Dunn B. Mesoporous indium tin oxide (ITO) films. *Thin Solid Films* 2006;515:790.
- [81] Rohlfing DF, Brezesinski T, Rathouský J, Feldhoff A, Oekermann T, Wark M, Smarsly B. Transparent conducting films of indium tin oxide with 3D mesopore architecture. *Advanced Materials* 2006;18:2980.
- [82] Fattakhova-rohlfing D, Brezesinski T, Smarsly B. Template-assisted preparation of films of transparent conductive indium tin oxide. *Superlattices and Microstructures* 2008;44:686.
- [83] Königer T, Münstedt H. Influence of polyvinylpyrrolidone on properties of flexible electrically conducting indium tin oxide nanoparticle coatings. *Thin Solid Films* 2009;44:2736.
- [84] Maksimenko I, Gross M, Königer T, Münstedt H, Wellmann PJ. Conductivity and adhesion enhancement in low-temperature processed indium tin oxide/polymer nanocomposites. *Thin Solid Films* 2010;518:2910.
- [85] Asakuma N, Fukui T, Toki M, Imai H. Low-temperature synthesis of ito thin films using an ultraviolet laser for conductive coating on organic polymer substrates. *Journal of Sol-Gel Science and Technology* 2003;27:91.
- [86] Lee JM, Choi BH, Ji MJ, An YT, Park JH, Kwon JH, Ju BK. Effect of barrier layers on the properties of indium tin oxide thin films on soda lime glass substrates. *Thin Solid Films* 2009;517:4074.
- [87] Hong S, Han J. Indium tin oxide (ITO) thin film fabricated by indium–tin–organic sol including ITO nanoparticle. *Current Applied Physics* 2006;6:206.
- [88] Ederth J, Heszler P, Granqvist AH. Indium tin oxide films made from nanoparticles: models for the optical and electrical properties. *Thin Solid Films* 2003;445:199.
- [89] Ederth J, Johnsson P, Niklasson GA, Hoel A, Heszler P, Granqvist CG, Van Doorn AR, Jongorius MJ, Burgard D. Electrical and optical properties of thin films consisting of tin-doped indium oxide nanoparticles. *Physical Review B* 2003;68:1.
- [90] Puetz J, Al-Dahoudi N, Aegerter MA. Processing of transparent conducting coatings made with redispersible crystalline nanoparticles. *Advanced Engineering Materials* 2004;6:733-737.

- [91] Ederth J, Hultaker A, Niklasson GA, Heszler P, Van Doorn AR, Jongerius MJ, Burgard D, Granqvist CG. Thin porous indium tin oxide nanoparticle films: effects of annealing in vacuum and air. *Applied Physics A* 2005;81:1363.
- [92] Tsai MS, Wang CL, Hon MH. The preparation of ITO films via a chemical solution deposition process. *Surface and Coatings Technology* 2003;172:95.
- [93] Kim H, Wang S, Park H, Chang H, Jeon H, Hill R. Study of Ag nanoparticles incorporated SnO₂ transparent conducting films by photochemical metal–organic deposition. *Thin Solid Films* 2007;516:198-202.
- [94] Wu KY, Wang CC, Chen DH. Preparation and conductivity enhancement of al-doped zinc oxide thin films containing trace ag nanoparticles by the sol–gel process. *Nanotechnology* 2007;18:5604.
- [95] Houg B, Huang C. Structure and properties of ag embedded aluminum doped zno nanocomposite thin films prepared through a sol–gel process. *Surface and Coatings Technology* 2006;201:3188.
- [96] Tao XY, Fsaifes I, Koncar V, Dufour C, Lepers C, Hay L, Capoen B, Bouzaoui M. CO₂ laser-induced crystallization of sol–gel-derived indium tin oxide films. *Applied Physics A* 2009;96:741.
- [97] Seki S, Sawada Y, Nishide T. Indium–tin-oxide thin films prepared by dip-coating of indium diacetate monohydroxide and tin dichloride. *Thin Solid Films* 2001;388:22.
- [98] Yamamoto O, Sasamoto T, Inagaki M. Indium tin oxide thin films prepared by thermal decomposition of ethylene glycol solution. *Journal of Materials Research* 2011;7:2488.
- [99] Psuja P, Streck W. Fabrication of indium tin oxide (ITO) thin films by spin-coating deposition method. *Proceedings of SPIE* 2007;6674:1.
- [100] Okuya M, Ito N, Shiozaki K. ITO thin films prepared by a microwave heating. *Thin Solid Films* 2007;515:8656.
- [101] Li ZH, Ke YP, Ren DY. Effects of heat treatment on morphological, optical and electrical properties of ITO films by sol-gel technique. *Transactions of Nonferrous Metals Society of China* 2008;18:366.
- [102] Liu J, Wu D, Zeng S. Influence of temperature and layers on the characterization of ito films. *Journal of Materials Processing Technology* 2009;209:3943.

- [103] Zhang J, Hu JQ, Zhu FR, Gong H, O'Shea SJ. Quartz crystal microbalance coated with sol-gel-derived thin films as gas sensor for no detection. *Sensors* 2003;3:404.
- [104] Su C, Sheu TK, Chang YT, Wan MA, Feng MC, Hung WC. Preparation of ITO thin films by sol-gel process and their characterizations. *Synthetic Metals* 2005;153:9.
- [105] De A, Biswas PK, Manara J. Study of annealing time on sol-gel indium tin oxide films on glass. *Materials Characterization* 2007;58:629.
- [106] Alam MJ, Cameron DC. Investigation of annealing effects on sol-gel deposited indium tin oxide thin films in different atmospheres. *Thin Solid Films* 2002;421:76.
- [107] Dismukes JP, Jones LH, Bailar JC. The measurement of metal-ligand bond vibrations. *Journal of Physical Chemistry* 1961;65:792.
- [108] Nakamoto K. *Infrared and raman spectra of inorganic and coordination compounds*. 4th ed. New York: John Wiley & Sons; 1986.
- [109] Pramanik NC, Das S, Biswas PK. The effect of Sn (IV) on transformation of co-precipitated hydrated In (III) and Sn (IV) hydroxides to indium tin oxide (ITO) powder. *Materials Letters* 2002;56:671.
- [110] Rey JFQ, Plivelic TS, Rocha RA, Tadokoro SK, Torriani I, Muccillo ENS. Synthesis of In₂O₃ nanoparticles by thermal decomposition of a citrate gel precursor. *Journal of Nanoparticle Research* 2005;7:203.
- [111] Diaz-Acosta I, Baker J, Cordes W, Pulay P. Calculated and experimental geometries and infrared spectra of metal tris-acetylacetonates: vibrational spectroscopy as a probe of molecular structure for ionic complexes: part I. *The Journal of Physical Chemistry* 2001;105:238-244.
- [112] Yu D, Yu W, Wang D, Qian Y. Structural, optical, and electrical properties of indium tin oxide films with corundum structure fabricated by a sol-gel route based on solvothermal reactions. *Thin Solid Films* 2002;419:166.
- [113] Zhang J, Hu J, Zhu ZQ, Gong H, O'Shea SJ. Quartz crystal microbalance coated with sol-gel-derived indium-tin oxide thin films as gas sensor for no detection. *Colloids and Surfaces A: Physicochemical and Engineering Aspects* 2004;236:23.
- [114] Lee HC, Park OO. Electron scattering mechanisms in indium-tin-oxide thin films: grain boundary and ionized impurity scattering. *Vacuum* 2004;75:275.

[115] Scherer GW. Sintering of sol-gel films. *Journal of Sol-Gel Science and Technology* 1997;8:353.